Early Cretaceous construction of a structural culmination, Eureka, Nevada, U.S.A.: Implications for out-of-sequence deformation in the Sevier hinterland

Sean P. Long[1,*], Christopher D. Henry[1], John L. Muntean[1], Gary P. Edmondo[2], and Elizabeth J. Cassel[3]
[1]*Nevada Bureau of Mines and Geology, Mail Stop 178, University of Nevada, Reno, Nevada 89557, USA*
[2]*Timberline Resources Corporation, 101 East Lakeside, Coeur D'Alene, Idaho 83814, USA*
[3]*Department of Geological Sciences, University of Idaho, P.O. Box 443022, Moscow, Idaho 83844, USA*

ABSTRACT

Assessing temporal relationships between foreland and hinterland deformation in fold-thrust belts is critical to understanding the dynamics of orogenic systems. In the western U.S. Cordillera, the central Nevada thrust belt (CNTB) has been interpreted as a hinterland component of the Sevier fold-thrust belt in Utah. However, imprecise timing constraints on CNTB deformation have hindered evaluation of space-time patterns of strain partitioning between these two thrust systems. To address this problem, new 1:24,000-scale geologic mapping and balanced cross sections are presented through the CNTB near Eureka, Nevada, in conjunction with industry drill-hole data, conodont age determinations, and $^{40}Ar/^{39}Ar$ and U-Pb ages from volcanic, intrusive, and sedimentary rocks.

Our mapping redefines the first-order structures and deformation geometry of the CNTB at the latitude of Eureka. Contractional structures include two north-striking, east-vergent thrust faults, the Prospect Mountain thrust and Moritz-Nager thrust, which are connected as the same fault in cross section, several north-striking map-scale folds, and a Cambrian over Silurian relationship observed in multiple drill holes, corresponding to repetition of ~2–2.5 km of stratigraphy, that defines the blind Ratto Canyon thrust. Two distinct sets of normal faults cut the contractional structures, and are overlapped by a regional late Eocene (ca. 37 Ma) subvolcanic unconformity. Retrodeformation of both sets of normal faults reveals the existence of the Eureka culmination, a 20-km-wide, 4.5-km-tall anticline with limb dips of 25°–35°, that can be traced for ~100 km north-south on the basis of Paleogene erosion levels. The culmination is interpreted as a fault-bend fold that formed from ~9 km of eastward displacement of the Ratto Canyon thrust sheet over a buried footwall ramp.

The type exposure of the Early Cretaceous (Aptian) Newark Canyon Formation (NCF) is preserved on top of Mississippian, Pennsylvanian, and Permian rocks on the eastern limb of the Eureka culmination. We propose that the NCF was deposited in a piggyback basin on the eastern limb of the culmination as it grew, which is consistent with published east-directed paleocurrents and provenance data suggesting derivation from proximal late Paleozoic subcrop units. Syncontractional deposition of the NCF is used to define the probable Aptian construction of the Eureka culmination and associated slip on the Ratto Canyon thrust at depth. After deposition, the NCF continued to be folded during late-stage growth of the culmination.

Aptian deformation in the CNTB at Eureka postdated migration of the Sevier thrust front into Utah by at least ~10 m.y. and possibly as much as ~30 m.y., and therefore represents out-of-sequence hinterland deformation. CNTB deformation was coeval with emplacement of the Canyon Range thrust sheet in the type-Sevier thrust belt in western Utah, and may represent internal shortening of this orogen-scale thrust sheet that acted to promote further eastward translation.

INTRODUCTION

The Jurassic–Paleogene North American Cordillera is the type example of an ancient orogen that formed between converging continental and oceanic plates (e.g., Armstrong, 1968; Burchfiel and Davis, 1975; Oldow et al., 1989; Allmendinger, 1992; Burchfiel et al., 1992; DeCelles, 2004; Dickinson, 2004). In the western interior United States, major components of the Cordillera include the Sierra Nevada magmatic arc in California, and a broad retroarc region across Nevada and western Utah in which most crustal shortening was accommodated (Fig. 1). The retroarc region has been divided into distinct tectonic zones, including the Jurassic Luning-Fencemaker thrust belt in western Nevada (e.g., Oldow, 1983, 1984; Wyld, 2002) and the Cretaceous frontal Sevier thrust belt in Utah (e.g., Armstrong, 1968; Burchfiel and Davis, 1975; Royse et al., 1975; Villien and Kligfield, 1986; DeCelles and Coogan, 2006). Between these two loci of Cordilleran crustal shortening is a broad hinterland region that underwent distinct Jurassic and Cretaceous magmatic, metamorphic, and shortening events, although the timing and relative magnitude of Jurassic versus Cretaceous deformation within this region are debated (e.g., Armstrong, 1972; Allmendinger and Jordan, 1981; Gans and Miller, 1983; Miller et al., 1988; Speed et al., 1988; Thorman et al., 1991, 1992; Bjerrum and Dorsey, 1995; Miller and Hoisch, 1995; Camilleri and Chamberlain, 1997; Taylor et al., 2000; Wyld et al., 2001; Martin et al., 2010; Greene, 2014).

One debate centers on the timing of deformation in the central Nevada thrust belt (CNTB), defined by Taylor et al. (1993) as a series of dominantly east-vergent thrust faults and folds exposed between the towns of Alamo and Eureka, Nevada (Fig. 1). Thrust systems in the southern part of the CNTB connect southward with thrust faults of the Sevier belt in southern Nevada (Bartley and Gleason, 1990; Armstrong and Bartley, 1993; Taylor et al., 1993, 2000; Long, 2012), implying an overlap in deforma-

*Corresponding author: splong@unr.edu

Geosphere; June 2014; v. 10; no. 3; p. 564–584; doi:10.1130/GES00997.1; 13 figures; 1 table; 3 plates; 1 supplemental file.
Received 24 October 2013 ♦ Revision received 25 February 2014 ♦ Accepted 8 April 2014 ♦ Published online 25 April 2014

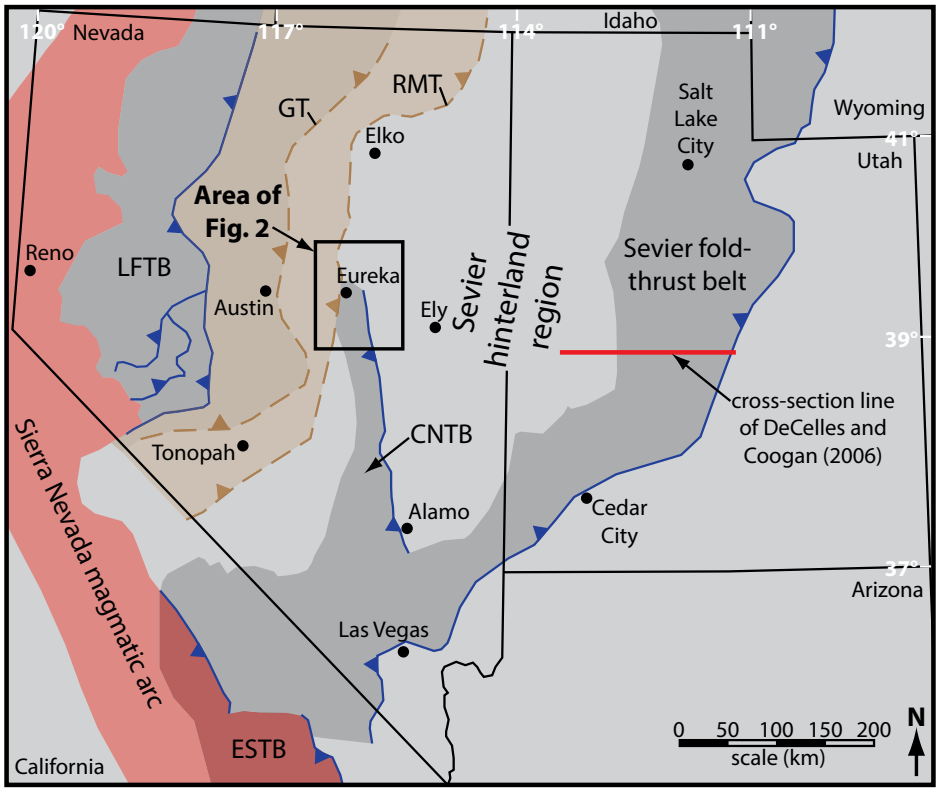

Figure 1. Map showing Paleozoic and Mesozoic thrust systems of Nevada, Utah, and southeast California (modified from Long, 2012). Approximate deformation fronts of Paleozoic and Mesozoic thrust systems are shown in brown and blue, respectively, and spatial extents are shaded. Location of Sierra Nevada magmatic arc is from Van Buer et al. (2009) and DeCelles (2004). Abbreviations: GT—Golconda thrust; RMT—Roberts Mountains thrust; LFTB—Luning-Fencemaker thrust belt; CNTB—central Nevada thrust belt; ESTB—Eastern Sierra thrust belt.

tion timing between these two thrust systems. However, on the basis of crosscutting relationships, southern CNTB thrust faults can only be broadly bracketed between the Pennsylvanian and the Late Cretaceous (Taylor et al., 2000), hindering evaluation of space-time patterns of strain partitioning between the CNTB and the Sevier thrust belt.

This problem is compounded in the northern part of the CNTB, near the town of Eureka (Fig. 1), an area that has been interpreted as occupying a zone of thrust faults and folds in several generations of studies (e.g., Nolan et al., 1971, 1974; Taylor et al., 1993; Carpenter et al., 1993). Here dating of contractional deformation has been hindered by varying interpretations of the style and geometry of large-offset faults (e.g., Nolan, 1962; Nolan et al., 1971, 1974; Roeder, 1989; Carpenter et al., 1993; Ransom and Hansen, 1993; Taylor et al., 1993; Lisenbee et al., 1995; Lisenbee, 2001a) and their relationships to the Early Cretaceous Newark Canyon Formation (NCF), a sedimentary unit preserved in several isolated exposures in the region (Nolan et al., 1971, 1974; Hose, 1983; Vandervoort and Schmitt, 1990) (Fig. 2). Contractional deformation in the Eureka region has been proposed to be bracketed between the Permian and Early Cretaceous (Nolan, 1962; Taylor et al., 1993; Lisenbee et al., 1995), to be dominantly Early Cretaceous, coeval with deposition of the NCF (Vandervoort and Schmitt, 1990; Carpenter et al., 1993; Ransom and Hansen, 1993), and possibly to be as young as Late Cretaceous (Vandervoort and Schmitt, 1990; Taylor et al., 1993). These varying interpretations are further compounded by complex, overprinting extensional deformation, which has hindered reconstruction of the preextensional structural geometry.

The purpose of this paper is to present a new structural and geometric definition of the CNTB at the latitude of Eureka. To achieve this goal, a new 1:24,000-scale geologic map of the northern Fish Creek Range and southern Diamond Mountains is presented (Plate 1; Fig. 2), along with deformed and restored cross sections (Plates 1–3), industry drill-hole data, conodont age determinations, and U-Pb and $^{40}Ar/^{39}Ar$ geochronology of volcanic, intrusive, and sedimentary rocks. These data facilitate redefinition of the first-order structures that compose the CNTB, and reconstruction of the regional preextensional deformation geometry. In addition, a structural model is presented that relates deposition in the type-NCF basin to CNTB deformation, including growth of a regional-scale anticline and associated motion on a thrust fault at depth, thereby placing the CNTB and NCF into the broader spatiotemporal framework of Sevier deformation and synorogenic deposition. This work is aided by recent U-Pb geochronology in the NCF type section (Druschke et al., 2011) and a recent synthesis of the timing and magnitude of crustal shortening accommodated in the type-Sevier thrust belt at the latitude of our study area (DeCelles and Coogan, 2006), both of which facilitate assessment of temporal relationships between foreland and hinterland shortening. Implications of this work for the dynamics of the Cordilleran orogenic wedge are then explored.

GEOLOGIC SETTING AND STRATIGRAPHY

Eastern Nevada has occupied a diverse range of tectonic settings that have evolved through the Phanerozoic (e.g., Dickinson, 2006). In the study area this tectonic development is preserved in a rock record that spans the Paleozoic, Mesozoic, and Tertiary (Plate 1; Fig. 3).

Paleozoic

From the late Neoproterozoic to the Devonian, the Cordilleran passive margin sequence, a westward-thickening section of clastic and carbonate rocks, was deposited on the rifted North American continental shelf in what is now eastern Nevada and western Utah (e.g., Stewart and Poole, 1974). Eureka was situated near the distal, western margin of the shelf (Cook and Corboy, 2004). In the study area the exposed part of the passive margin sequence is 4.7 km thick, and consists of lower Cambrian clastic rocks, including the Prospect Mountain Quartzite, and a middle Cambrian to Devonian section dominated by limestone and dolomite, with lesser quartzite and shale (Fig. 3) (e.g., Palmer, 1960; Nolan, 1962; Ross, 1970; Nolan et al., 1974).

During the Mississippian, the Roberts Mountains allochthon, composed of distal slope and basinal sediments, was thrust to the east over the western edge of the continental shelf during the Antler orogeny (e.g., Burchfiel and Davis, 1975; Dickinson, 1977; Speed and Sleep, 1982). Eureka is immediately to the east of the Antler thrust front (Fig. 1), but was the site of

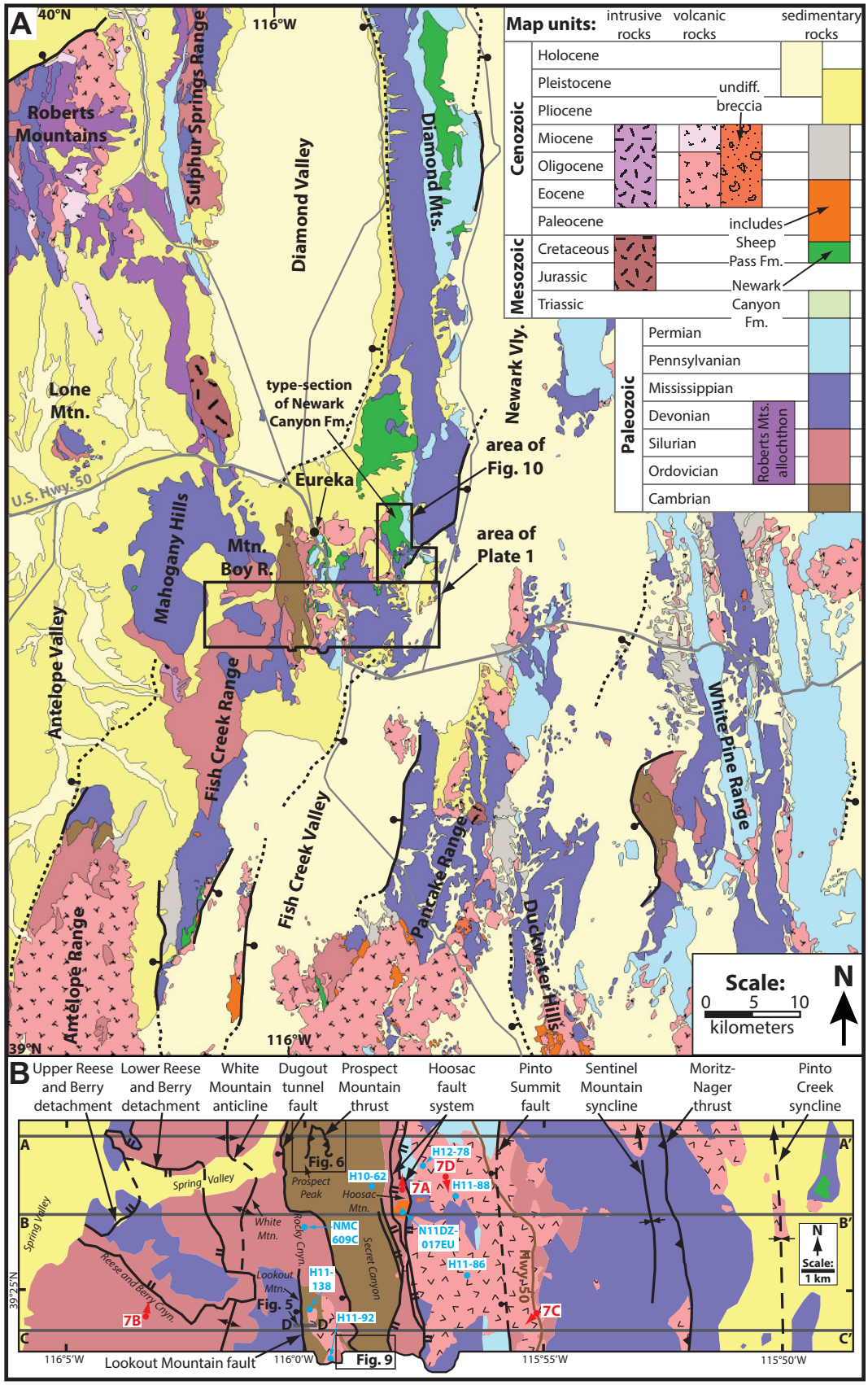

Figure 2. (A) Geologic map of part of east-central Nevada; geology simplified from Crafford (2007) and Quaternary faults simplified from the U.S. Geological Survey (2006) fault and fold database. Vly.—valley; R—range; Mts.—mountains; undiff—undifferentiated. (B) Simplified version of Plate 1 with the same map units as A, showing geographic names relevant to discussion in text, locations of structures, and cross-section lines. Red dots with arrows show location and view direction of annotated photographs in Figure 7, and blue dots show locations of U-Pb and $^{40}Ar/^{39}Ar$ samples.

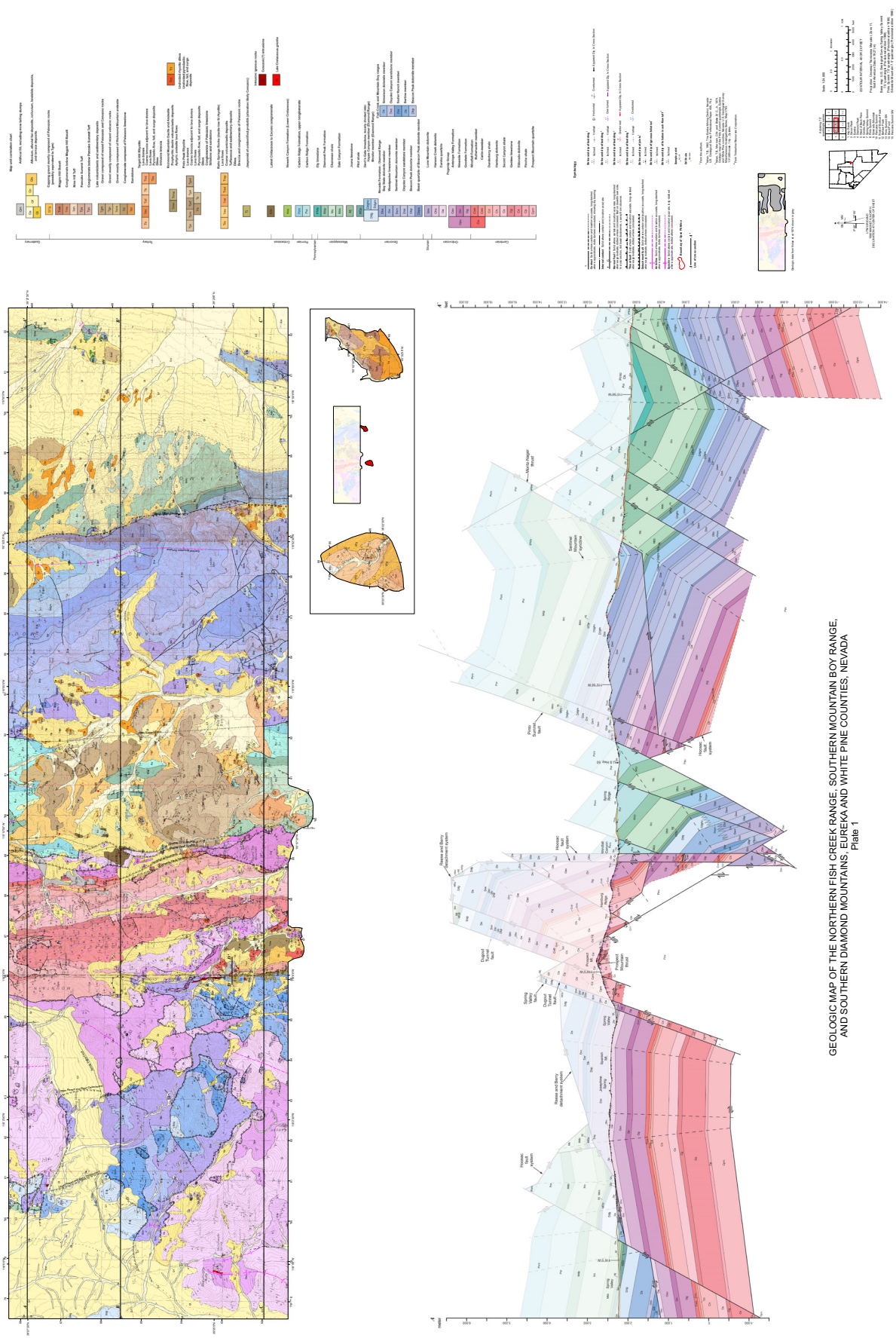

Plate 1. 1:24,000-scale geologic map of northern Fish Creek Range, southern Mountain Boy Range, and southern Diamond Mountains, cross-section A–A′, and unit correlation chart, modified from Long et al. (2012). Translucent areas above modern erosion surface on cross section represent eroded rock. If you are viewing the PDF of this paper or reading it offline, please visit http://dx.doi.org/10.1130/GES00997.S2 or the full-text article on www.gsapubs.org to view the full-sized version of Plate 1.

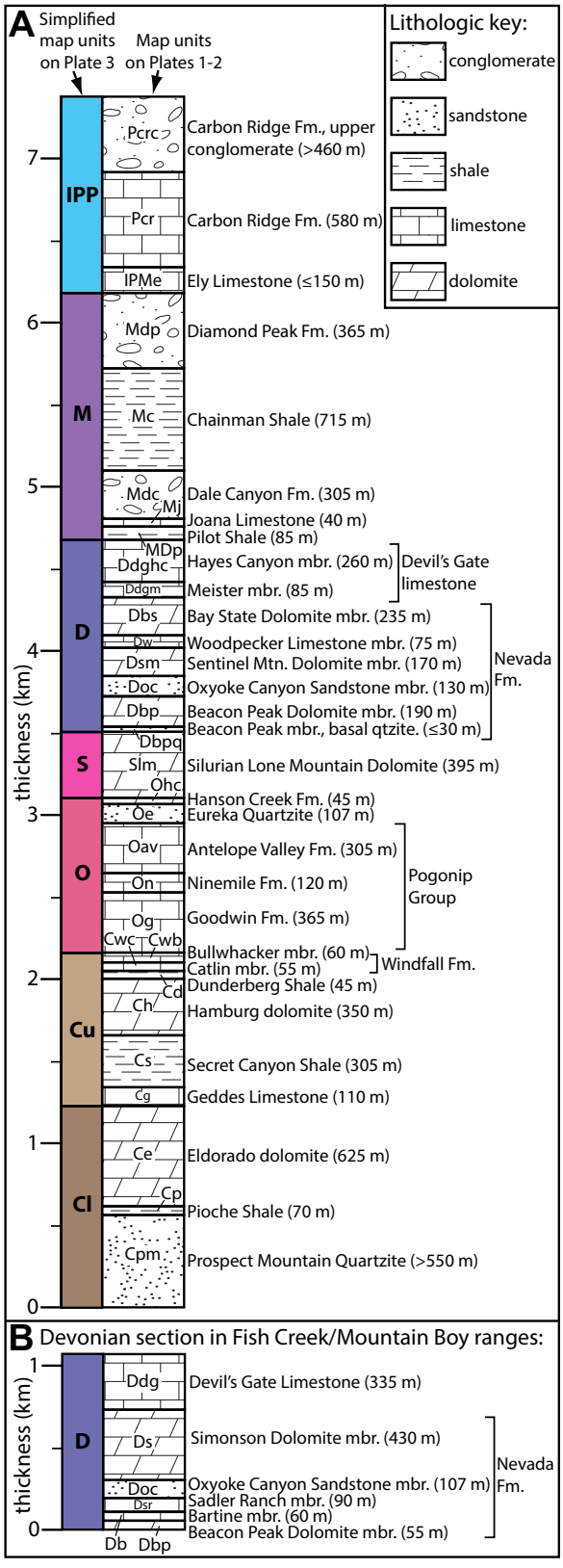

Figure 3. (A) Stratigraphic column of Paleozoic rock units in the study area. Column on right shows map unit divisions used in Plates 1 and 2, and column on left shows simplified unit divisions used on balanced cross sections in Plate 3 (Cl—lower Cambrian, Cu—upper Cambrian, O—Ordovician, S—Silurian, D—Devonian, M—Mississippian, IPP—Pennsylvanian and Permian). (B) Devonian stratigraphy of Fish Creek and Mountain Boy Ranges (note: stratigraphic column in A shows Devonian stratigraphy of Diamond Mountains).

synorogenic deposition of Mississippian clastic sediments that were sourced from the Roberts Mountains allochthon (e.g., Poole, 1974; Smith and Ketner, 1977; Poole and Sandberg, 1977). In the study area the Mississippian section consists of 1.5 km of conglomerate, sandstone, and shale, including the Chainman Shale and Diamond Peak Formation (Fig. 3) (e.g., Brew, 1961a, 1961b, 1971; Stewart, 1962; Nolan et al., 1974).

During the Pennsylvanian and early Permian, eastern Nevada underwent a protracted series of deformation and erosion events recorded by unconformity-bound packages of carbonate and clastic rocks (e.g., Trexler et al., 2004). In the study area, the Pennsylvanian–Permian section consists of 1.3 km of limestone and conglomerate, including the Ely Limestone and Carbon Ridge Formation (Fig. 3).

Mesozoic

Across eastern Nevada and western Utah, a regional unconformity places Tertiary and in some places Cretaceous rocks over Paleozoic to Triassic rocks (e.g., Armstrong, 1972; Gans and Miller, 1983; Long, 2012). This unconformity records the net erosion that occurred during Jurassic and Cretaceous deformation within the Sevier hinterland and Cretaceous uplift of the hinterland that accompanied crustal thickening in the frontal Sevier thrust belt (e.g., Coney and Harms, 1984; DeCelles, 2004; Long, 2012).

In the Eureka region, the Mesozoic section is represented by the Early Cretaceous NCF, which is preserved in a series of isolated exposures in the Diamond Mountains and Fish Creek Range (Fig. 2) (Nolan et al., 1971, 1974; Hose, 1983). The NCF is only exposed in the northeast corner of the map area (Plate 1), where it overlies Mississippian and Pennsylvanian rocks. However, the NCF type section is exposed 1–5 km north of the map area in the Diamond Mountains (Fig. 2), and consists of ~500 m of conglomerate, mudstone, and limestone (Vandervoort, 1987). Rocks in the type section exposure are interpreted to record fluvial and lacustrine deposition (Vandervoort and Schmitt, 1990). The NCF type section has yielded Aptian–Albian fossil fish, ostracods, and nonmarine mollusks (MacNeil, 1939; Fouch et al., 1979). A ca. 116 Ma U-Pb zircon age obtained from an air-fall tuff in the type section defines an Aptian deposition age, and a ca. 122 Ma youngest U-Pb detrital zircon age population obtained from sandstone in the type section defines an Aptian maximum deposition age (Druschke et al., 2011).

One other rock unit of possible Mesozoic age in the study area is a conglomerate that unconformably overlies Ordovician, Mississippian, and Permian rocks on Hoosac Mountain (Fig. 2;

Plate 1). Nolan et al. (1974) mapped this conglomerate as the NCF. However, the conglomerate contains detrital zircon that have a ca. 72 Ma youngest U-Pb age population, defined by 3 concordant grains that overlap within error (sample NV11DZ-017EU; Fig. 4; see Supplemental File[1] for methods, concordia plots, and data from individual analyses), that defines a Late Cretaceous maximum depositional age (e.g., Dickinson and Gehrels, 2009). The conglomerate is overlain by late Eocene dacite, defining a minimum deposition age.

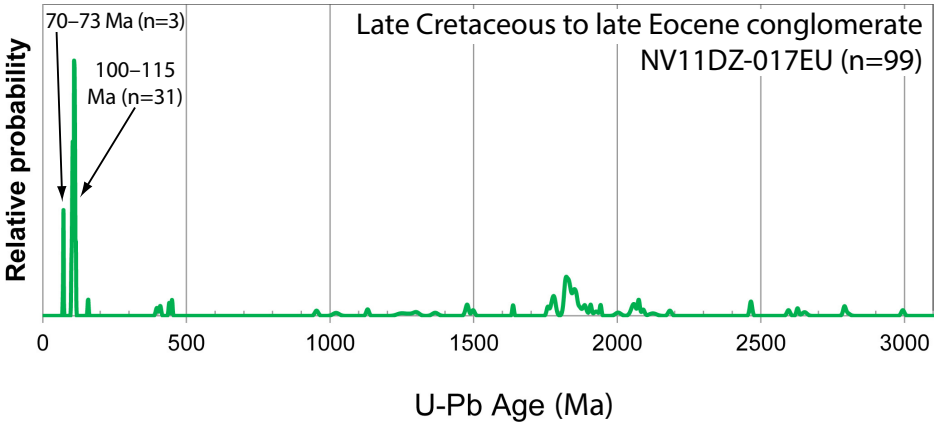

Figure 4. U-Pb detrital zircon age spectrum of Late Cretaceous to late Eocene conglomerate sample NV11DZ-017EU collected on Hoosac Mountain (location: 39.48535°N, 115.94587°W; Fig. 2; Plate 1). Graph is a relative probability plot, which represents the sum of probability distributions from ages and corresponding errors (input errors are 2σ) for all analyses. Cretaceous age populations are labeled. Refer to Supplemental File (see footnote 1) for discussion of methods, concordia plots, and data from individual analyses.

Tertiary

Nevada was the site of the Great Basin ignimbrite flareup, an episode of silicic volcanism that swept from northeast to southwest across the state from the late Eocene to the early Miocene (e.g., Coney, 1978; Armstrong and Ward, 1991; Best and Christiansen, 1991; Henry, 2008; Best et al., 2009). Ignimbrite flareup rocks in the Eureka region include late Eocene silicic lavas, tuffs, shallow intrusive rocks, and associated volcaniclastic and sedimentary rocks. Volcanic rocks are concentrated in the central and northeast parts of the map area (Fig. 2; Plate 1), and include the Pinto Peak and Target Hill rhyolite dome systems, Ratto Springs dacite, and Richmond Mountain andesite. K-Ar ages of these volcanic rocks range between ca. 37 and 33 Ma (Nolan et al., 1974), and new $^{40}Ar/^{39}Ar$ dates (Table 1; see Supplemental File [see footnote 1] for age spectra, inverse isochron plots, and data from individual analyses) show that the oldest volcanic rocks are 37.4 Ma (late Eocene).

From the Neogene to the present, much of Nevada and western Utah has been the site of regional extensional tectonism. Widespread, large-magnitude, upper crustal extension began in the early Miocene (ca. 17.5 Ma) (e.g., Dickinson, 2006), and by ca. 10 Ma either transitioned into, or was followed by a separate episode of, lower magnitude extension that formed the modern Basin and Range topography (e.g., Dickinson, 2002; Colgan and Henry, 2009). However, although more local in scale, evidence for pre–middle Miocene extension in areas of Nevada and Utah has also been presented, including tectonic denudation of metamorphic core complexes (e.g., Snoke and Miller, 1988; Hodges and Walker, 1992; Camilleri and Chamberlain, 1997; McGrew et al., 2000), and development of latest Cretaceous to Eocene extensional basins (e.g., Vandervoort and Schmitt, 1990; Potter et al., 1995; Druschke et al., 2009a, 2009b).

STRUCTURES AND DEFORMATION TIMING CONSTRAINTS

The Eureka area has experienced a multiphase tectonic history of contractional deformation complexly overprinted by extensional deformation. Interpretations of the style, geometry, and origin of many large-offset faults in the Fish Creek Range and Diamond Mountains have varied widely in previous studies (e.g., Nolan et al., 1971, 1974; Carpenter et al., 1993; Ransom and Hansen, 1993; Taylor et al., 1993; Lisenbee, 2001b), resulting in significant disagreement over deformation geometry and timing. In the following sections, map-scale faults and folds are described, along with observations that support interpretations of their style and geometry, and field relationships that bracket their motion timing. These observations are used to support construction of three 1:24,000-scale deformed cross sections (Plates 1 and 2), and three 1:100,000-scale deformed and restored balanced cross sections (Plate 3). The balanced cross sections are based on the 1:24,000-scale cross sections, but with simplified Paleozoic stratigraphy (Fig. 3), and with faults with <300 m of offset omitted. The top row of Plate 3 shows the modern, deformed geometry, and the bottom row shows a partially restored geometry, with motions on extensional faults retrodeformed. Angles, line lengths, and offsets on faults were matched between the deformed and restored cross sections (e.g., Dahlstrom, 1969).

The dip directions of faults were determined by the interactions of fault traces with topography in Plate 1, and quantitative estimates of the dip angles of faults were determined using three-point problems on fault traces (see Table SM4 in the Supplemental File [see footnote 1] for supporting data). It was assumed that the fault dip angle estimated at the modern erosion surface stays the same both above and below the modern erosion surface. Apparent dips of supporting attitude measurements were projected onto the cross sections (Plates 1 and 2), and areas of similar apparent dip were divided into dip domains. Boundaries between adjacent dip domains were treated as kink surfaces (e.g., Suppe, 1983), their orientations determined by bisecting the interlimb angle. Division of areas of the cross sections into dip domains, combined with quantitative constraints on fault dip angles, allowed estimation of the cutoff angles that strata make with faults at the modern erosion surface. All offset estimates listed in the following for specific faults were measured from the 1:24,000-scale cross sections in Plates 1 and 2, by measuring the displacement of matching hanging-wall and footwall cutoffs across the structure. Additional details on fault and fold geometry, and justifications for individual decisions made in drafting and retrodeforming the balanced cross sections are annotated in footnotes in Plate 3. All cross sections were drafted by hand.

Contractional Structures: The CNTB

On the eastern flank of Lookout Mountain (Fig. 2; Plate 1), drilling by Timberline Resources Corporation has revealed an older-

[1]Supplemental File. Zipped file containing 6 supplemental figures, 4 supplemental tables, supplemental ArcGIS files, and a supplemental text document. If you are viewing the PDF of this paper or reading it offline, please visit http://dx.doi.org/10.1130/GES00997.S1 or the full-text article on www.gsapubs.org to view the Supplemental File.

TABLE 1. $^{40}Ar/^{39}Ar$ AGES OF VOLCANIC ROCKS

Sample	Rock type	Mineral	Location	Latitude (°N)	Longitude (°W)						Ages (Ma)				
Single crystal				NAD27		wtd mn*	±2σ	n†	K/Ca	±2σ					
H11-86	rhyolite lava dome	sanidine	Pinto Peak	39.42009	115.94234	36.69	0.04	13/15	172	124					
Step heating						plateau	±2σ	%^{39}Ar§	steps	isochron	±2σ	$^{40}Ar/^{36}Ar$	±2σ	MSWD	total gas	±2σ
H11-88	dacite block-and-ash flow	biotite	Hoosac Canyon	39.44269	115.94683	37.40	0.02	93.3	7/12	37.37	0.06	308	8	1.70	37.50	0.04
H11-92	low-Si rhyolite lava	hornblende	Ratto Canyon	39.39799	115.98989	37.34	0.26	94.0	6/10	37.40	0.14	278	31	0.40	37.29	0.57
H10-62	dacite volcaniclastic	biotite	Rustler Pit	39.44545	115.97562	37.43	0.02	62.9	5/9	37.41	0.08	310	20	2.1	37.64	0.04
H11-138	dacite volcaniclastic	hornblende	Lookout Pit	39.41140	115.99837	37.28	0.21	100.0	6/6	37.31	0.10	276	45	0.38	37.27	0.38
H12-78	dacite volcaniclastic	plagioclase	Windfall Canyon	39.45139	115.95933	37.14	0.12	100.0	14/14	37.12	0.12	299	6	0.73	37.15	0.22

Note: NAD—North American Datum of 1927. MSWD—mean square of weighted deviates. All samples were analyzed at the New Mexico Geochronological Research Laboratory (methodology in McIntosh et al., 2003). Neutron flux monitor: Fish Canyon Tuff sanidine (FC-1). Assigned age: 28.201 Ma (Kuiper et al., 2008). Minerals were concentrated from crushed, sieved samples by standard magnetic and density techniques. Sanidine was leached with dilute HF to remove matrix. All samples were hand-picked to final purity. Decay constants after Min et al. (2000); λ_{total} (total ^{40}K decay constant) = 5.463 x 10^{-10} yr^{-1}. Isotopic abundances after Steiger and Jäger (1977); $^{40}K/K$ = 1.167 x 10^{-4}

*wtd mn = weighted mean, calculated by method of Samson and Alexander (1987).

†Number of single grains used in age calculation/total number of grains analyzed.

§%^{39}Ar = percentage of ^{39}Ar used to define plateau age.

over-younger relationship at depth, defined by Cambrian Geddes Limestone, and locally Cambrian Secret Canyon Shale, over Silurian Lone Mountain Dolomite (Fig. 5), corresponding to structural repetition of ~1800–2300 m of stratigraphy. This is interpreted as evidence for a large-throw thrust fault at depth, here named the Ratto Canyon thrust. The thrust has been intercepted in 5 drill holes over a north-south distance of 3 km, at depths between 350 and 450 m, and does not breach the modern erosion surface within the map area. In addition to lithologic logs of drill core, the existence of the Ratto Canyon thrust is corroborated by Silurian and Ordovician conodont age determinations from sampled footwall rocks (Fig. 5) (see Supplemental File [see footnote 1] for drill-hole lithologic logs and conodont age determination report).

On Prospect Mountain (Figs. 2 and 6), a ~10°E dipping fault with ~60° hanging-wall and footwall cutoff angles exhibits a top-to-the-east motion sense, and places older rocks over younger rocks. This fault was mapped as an unnamed thrust fault by Nolan (1962) and Nolan et al. (1974), and is here named the Prospect Mountain thrust. The thrust places Prospect Mountain Quartzite, Pioche Shale, and Eldorado Dolomite over Secret Canyon Shale (Fig. 6), and has ~1.0 km of top-to-the-east displacement (Plate 1). The Prospect Mountain thrust is cut by several normal faults (Fig. 6; Plate 1), including the Dugout Tunnel fault.

In the southern Diamond Mountains, the ~60°W dipping Moritz-Nager thrust (French, 1993) places Devonian rocks over Mississippian rocks (Plate 1; Fig. 2), and has an estimated top-to-the-east displacement between 1.0 and 1.8 km (Plates 1 and 2). In its hanging wall, the Sentinel Mountain syncline (Nolan et al., 1974) strikes parallel to the thrust trace. This upright, open syncline plunges 15°N and has a western limb that dips 20°E and an eastern limb that dips 20°–40°W. Both the Moritz-Nager thrust and the axis of the Sentinel Mountain syncline are overlapped by late Eocene tuff (Plate 1).

Though its axis is concealed under Quaternary sediment within much of the map area, the Pinto Creek syncline, originally described by Nolan et al. (1974) immediately north of our map area, is defined by outcrops of Devonian, Mississippian, and Pennsylvanian strata on the eastern flank of the Diamond Mountains, in the footwall of the Moritz-Nager thrust (Fig. 2; Plate 1). It is an upright, open syncline that plunges ~17°N, and has a western limb that dips 30°–60°NE and an eastern limb that dips 10°–20°NW.

A north-striking anticline axis can be traced along the topographic crest of the Fish Creek and Mountain Boy Ranges (Fig. 2; Plate 1). It is an upright, open fold, with a western limb that dips 10°–20°W and an eastern limb that dips 20°–30°E, here named the White Mountain anticline. The fold axis is cut by several normal faults (Plate 1), including the lower Reese and Berry detachment.

In summary, contractional structures in the map area include (1) two east-vergent thrust traces, the Prospect Mountain thrust and Moritz-Nager thrust, which are connected as the same structure in the cross sections (Plate 3) on the basis of the relative stratigraphic levels that they deform, similar offset magnitude (~1 km), and a lack of any surface-breaching thrust faults observed between their traces; (2) the Ratto Canyon thrust, which is defined by a Cambrian over Silurian relationship observed in drill holes (Fig. 5), corresponding to repetition of ~2–2.5 km of stratigraphy; and (3) three north-striking, upright, open folds, the White Mountain anticline, Sentinel Mountain syncline, and Pinto Creek syncline. The Prospect Mountain thrust and White Mountain anticline are cut by normal faults that predate late Eocene volcanism (see following discussion), and the Moritz-Nager thrust and Sentinel Mountain syncline are overlapped by late Eocene volcanic rocks.

Normal Faults

Normal faults in the map area can be divided into an older set, consisting of two oppositely verging fault systems with low (≤20°) cutoff angles to bedding, including the Hoosac fault system and Reese and Berry detachment system (Fig. 2; Plate 1), and a younger set of high dip-angle, down-to-the-west normal faults.

The down-to-the-east Hoosac fault system (Fig. 2; Plates 1–3) is an anastomosing series of ~70°–90°E dipping normal faults (Table SM4 in the Supplemental File [see footnote 1]) with low (typically ~20°) hanging-wall and footwall cutoff angles, and a cumulative offset of ~5 km. This fault system is modeled on the cross sections as a series of subvertical structures (Plates 1–3). The easternmost, master fault of the system places Mississippian and Permian rocks over Ordovician rocks (Fig. 7A; Plates 1–3), corresponding to an omission of ~2–3 km of stratigraphy, and a series of subsidiary faults west of the master fault deform Ordovician and late Cambrian rocks (Plate 1). The master fault has been interpreted as a steeply east dipping normal fault (Hague, 1892; Nolan et al., 1974) and a shallowly west dipping thrust fault (Nolan, 1962; Taylor et al., 1993; Lisenbee, 2001b) in previous studies. However, the map patterns of both the master fault and subsidiary faults (Plate 1), combined with multiple three-point problems calculated along their length

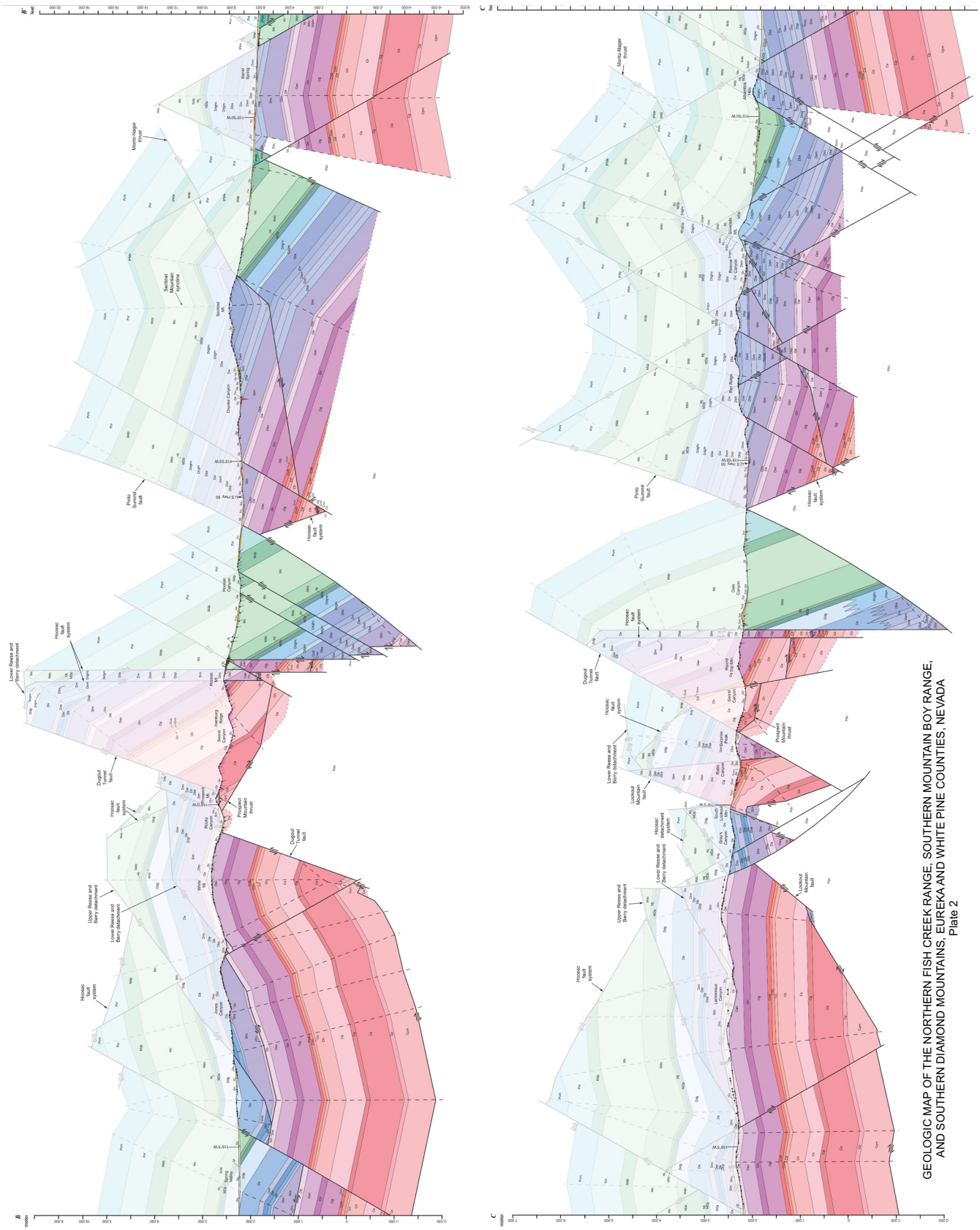

Plate 2. 1:24,000-scale cross-sections B–B′ and C–C′, modified from Long et al. (2012). Translucent areas above modern erosion surface represent eroded rock. If you are viewing the PDF of this paper or reading it offline, please visit http://dx.doi.org/10.1130/GES00997.S3 or the full-text article on www.gsapubs.org to view the full-sized version of Plate 2.

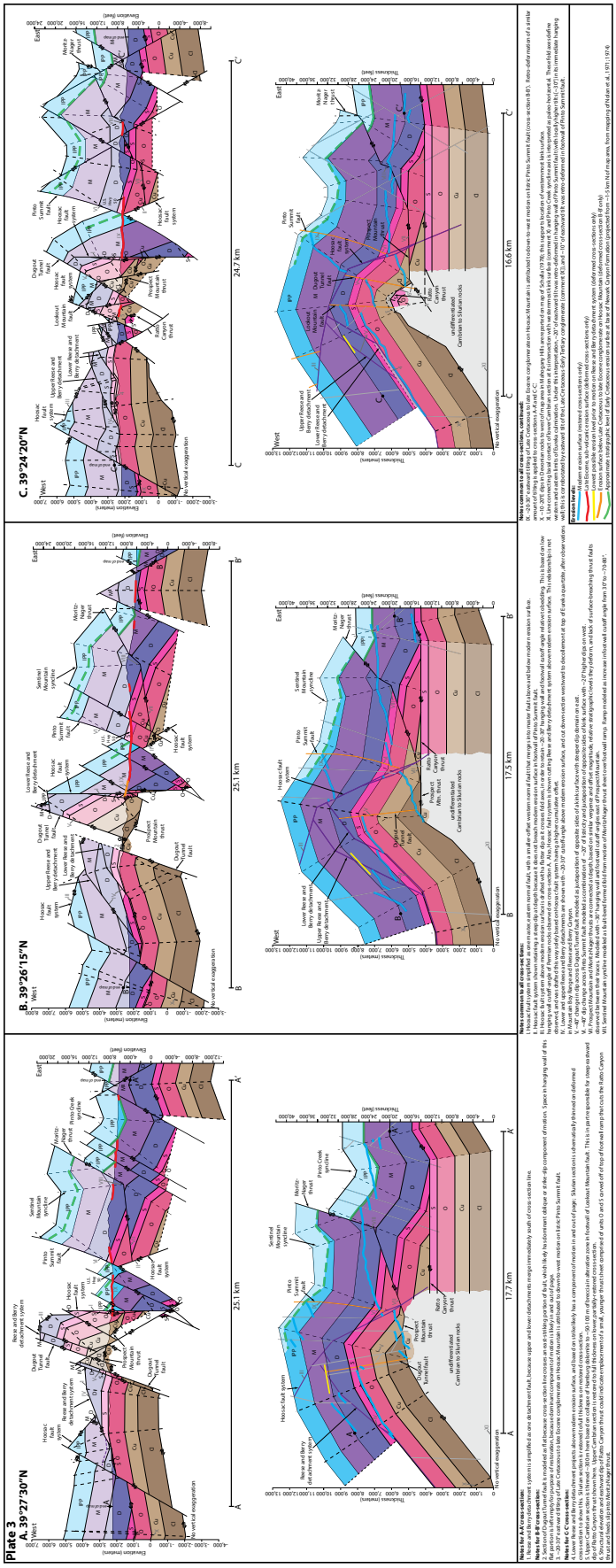

Plate 3. 1:100,000-scale balanced cross sections, with simplified Paleozoic stratigraphic divisions (Cl—lower Cambrian, Cu—upper Cambrian, O—Ordovician, S—Silurian, D—Devonian, M—Mississippian, IPP—Pennsylvanian and Permian; see Fig. 3), and all faults with <300 m of offset omitted. Quaternary and Tertiary rocks omitted for simplicity. Top row shows present-day deformed geometry, and bottom row shows partially restored geometry, with motion on extensional faults retrodeformed. Translucent areas above modern erosion surface represent eroded rock. Justifications for individual decisions made in drafting and retrodeforming cross sections are annotated. Lower right corner shows explanation of erosion levels. If you are viewing the PDF of this paper or reading it offline, please visit http://dx.doi.org/10.1130/GES00997.S4 or the full-text article on www.gsapubs.org to view the full-sized version of Plate 3.

(Table SM4 in the Supplemental File [see footnote 1]), demonstrate their steep eastward dip, which refutes the thrust fault interpretation. The easternmost two faults of the system are overlapped by late Eocene (ca. 36–37 Ma) dacite and rhyolite (Plate 1; Fig. 7A), and the westernmost two faults are cut by a late Eocene rhyolite dike (Plate 1). In addition, an angular unconformity at the base of the Late Cretaceous to late Eocene conglomerate on Hoosac Mountain overlaps the master Hoosac fault (Figs. 2 and 8; Plate 1).

The down-to-the-west Reese and Berry detachment system (Figs. 2 and 7B; Plate 1) consists of two ~10°–20°W dipping faults (Table SM4 in the Supplemental File [see footnote 1]) with hanging-wall and footwall cutoff angles typically between 0° and 20°. The lower detachment is developed along the top of the Ordovician Eureka Quartzite, which forms a footwall flat that can be traced for ~5 km across strike. Hanging-wall stratigraphic levels are typically in Silurian dolomite, indicating a maximum stratigraphic omission of 400 m. In addition, a bedding-parallel detachment fault that bounds the base of several klippen of Eureka Quartzite on White Mountain (Fig. 2; Plate 1) merges to the west with the lower detachment. The upper Reese and Berry detachment places Devonian dolomite over Silurian dolomite, omitting between 600 and 900 m of stratigraphy. In the Mountain Boy Range, the upper and lower detachments merge, and place Devonian rocks over Ordovician rocks, a stratigraphic omission of 1200–1500 m. Cumulative offset estimates for the Reese and Berry detachment system are 1.5–2.6 km in the Fish Creek Range and 4.7 km in the Mountain Boy Range (Plates 1 and 2). Similar low-cutoff-angle normal faults have been documented in other areas of the Fish Creek and Mountain Boy Ranges (Cowell, 1986; Lisenbee et al., 1995; Simonds, 1997; Lisenbee, 2000). Approximately 1.5 km south of the map area, the lower Reese and Berry detachment is cut by dikes of porphyritic granite, which are correlated with late Eocene (34.1 ± 1.5 Ma; Marvin and Cole, 1978) granite in the Mahogany Hills (Cowell, 1986).

The younger set of normal faults in the study area consists of three high-dip-angle (typically ~60°–70°), multiple-kilometer-throw (~2–4.5 km), down-to-the-west faults, including the Dugout Tunnel, Lookout Mountain, and Pinto Summit faults (Fig. 2; Plates 1–3). The Dugout Tunnel fault places shallowly east dipping Ordovician rocks over steeply east dipping Cambrian rocks, and has between 2500 and 2900 m of offset (Plates 1 and 2). The ~40° change in dip angle observed across the fault is modeled as juxtaposition of opposite sides of a kink surface (Plate 3). The Lookout Moun-

Figure 5. Cross sections through Lookout Mountain and Ratto Canyon, showing subsurface relationships revealed by industry drill holes (green lines). Locations of cross-section lines are shown in lower right inset (D–D′ is also shown in Plate 1 and Fig. 2). The Ratto Canyon thrust places Cambrian Geddes Limestone over Silurian Lone Mountain Dolomite. Silurian and Ordovician conodonts obtained from footwall rocks corroborate drill-hole lithologic interpretations (see Supplemental File [see footnote 1] for supporting lithologic logs and conodont age determinations for drill holes BH-0605 and BHSE-007C).

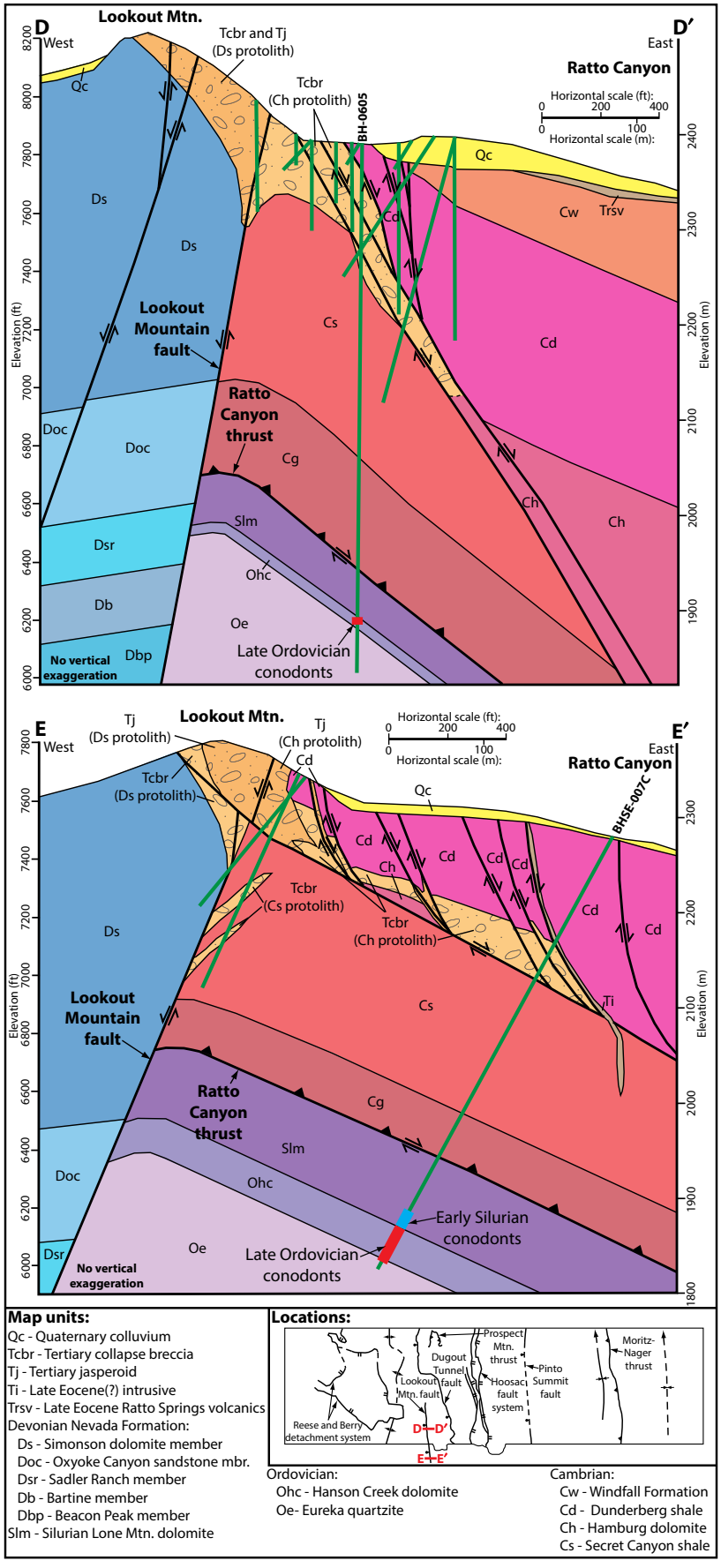

tain fault places Devonian rocks over Cambrian rocks, and has ~2000 m of down-to-the-west offset at Lookout Mountain (Plates 2 and 3). The Dugout Tunnel and Lookout Mountain faults are both overlapped by the late Eocene subvolcanic unconformity. In the footwall of the Lookout Mountain fault, the unconformity is on Cambrian rocks (Plate 1; Fig. 5), while modern erosion levels in its hanging wall preserve Devonian rocks. In addition, 3–6 km south of the map area, late Eocene volcanic rocks are mapped on both sides of the Lookout Mountain fault (Nolan et al., 1974; Cowell, 1986), with Cambrian erosion levels in the footwall and Devonian erosion levels in the hanging wall. In the footwall of the Dugout Tunnel fault, ~200 m south of the map area, Nolan et al. (1974) mapped late Eocene rhyolite in depositional contact over Cambrian rocks, while modern erosion levels in its hanging wall preserve strata as young as Ordovician (Fig. 9), indicating that the majority of motion had to be pre–late Eocene.

In Rocky Canyon (Fig. 2; Plate 1), the Dugout Tunnel fault places unmetamorphosed Ordovician limestone over Cambrian Secret Canyon Shale that is metamorphosed to hornfels, which is interpreted as contact metamorphism associated with intrusion of Late Cretaceous granite dikes at depth. This is supported by drill hole NMC609C, located 600 m to the southeast (Fig. 2; Plate 1), which drilled through Silurian and Ordovician dolomite, quartzite, and limestone before abruptly intercepting Secret Canyon Shale metamorphosed to hornfels and skarn. The metamorphism is spatially associated with numerous two-mica granite dikes intercepted in the drill hole. We present a new U-Pb zircon crystallization age of 86.1 ± 0.8 Ma (2σ) from a granite dike sampled from drill core (sample NMC609; see Supplemental File [see footnote 1] for methods, concordia plot, and

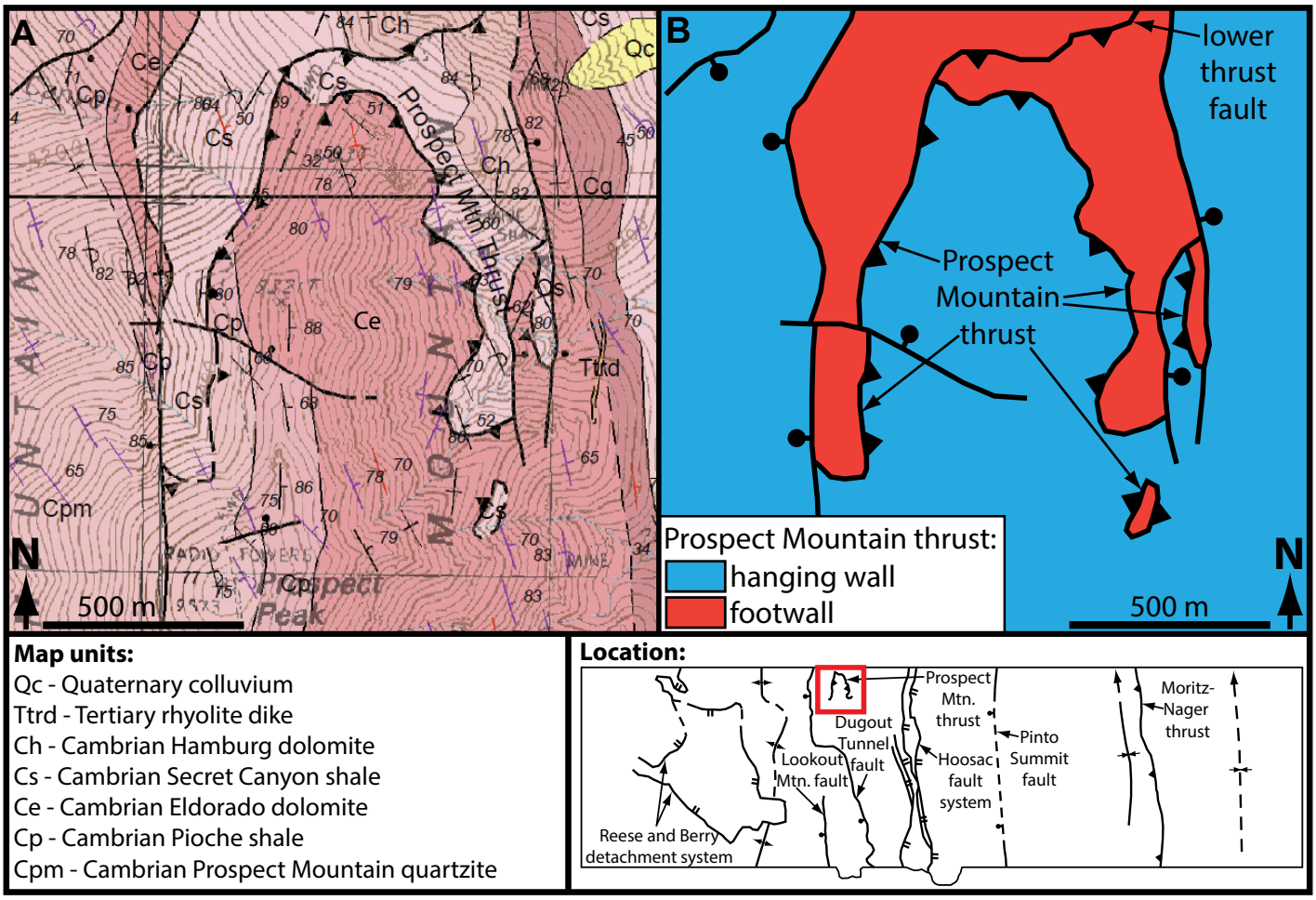

Figure 6. (A) Geologic map of the Prospect Mountain thrust (location shown in Fig. 2 and bottom right inset). Crosscutting normal faults drop trace of thrust below modern erosion surface on east and west. (B) Map of the same area as A, with hanging wall and footwall of Prospect Mountain thrust labeled.

data from individual analyses), which overlaps within error with the 84 ± 2 Ma age obtained by Barton (1987) from a granite dike sampled from the same drill hole. This indicates that the Dugout Tunnel fault cuts a contact aureole associated with a ca. 86 Ma intrusive system, which provides a maximum motion age. The Dugout Tunnel fault also cuts a detachment fault that bounds a klippe of Eureka Quartzite (Plate 1), which is correlated with the lower Reese and Berry detachment.

The Pinto Summit fault (Lisenbee, 2001b) places steeply east dipping Permian rocks on the west against shallowly east dipping Silurian rocks (Figs. 2 and 7C; Plates 1 and 2). The Pinto Summit fault has previously been interpreted as a down-to-the-east normal fault (Nolan et al., 1974; Lisenbee, 2001b) and a top-to-the-west reverse fault (Taylor et al., 1993). However, the map patterns of exposures on the north and south ends of the map area (Plate 1), combined with the results of three-point problems (Table SM4 in the Supplemental File [see footnote 1]), define a steep (~65°–75°) westward dip, which refutes the thrust fault interpretation. Offset estimates for the Pinto Summit fault range from 3.7 to 4.5 km (Plates 1–3). The fault is overlapped along most of its length by late Eocene volcanic rocks (Plate 1). Eastward tilting accompanying motion on the Pinto Summit fault is interpreted as the most likely mechanism for tilting the Late Cretaceous to late Eocene conglomerate on

Figure 7 (*on following page*). Annotated photographs (locations and view directions shown in Fig. 2, unit abbreviations shown in Plate 1). Dashed lines with dip numbers are apparent dip symbols. Red lines represent late Eocene unconformity. (A) Hoosac fault system viewed from Hoosac Mountain. Eastern, master fault places Permian rocks over Ordovician rocks, and westernmost fault omits units On and Oav. Late Eocene unconformity at base of unit Trsv overlaps master fault. Qu—undifferentiated Quaternary deposits. (B) Reese and Berry detachment system in Reese and Berry Canyon. Lower detachment occupies upper contact of Eureka Quartzite (Oe) for several kilometers across strike. Upper detachment places top of Devonian section (units Ds and Ddg) over lower Devonian rocks and Silurian rocks. Unit Du represents map units Dbp, Db, Dsr, and Doc undifferentiated. (C) Pinto Summit fault placing Permian rocks over Silurian rocks; note steeper dips in hanging wall. Late Eocene unconformity at base of unit Ttt overlaps the fault. (D) Late Eocene unconformity at base of Pinto Peak rhyolite (Tpr) and associated breccia (Tprx) and sedimentary rocks (Ts) is negligibly tilted, and overlies 60°–70°E dipping Mississippian and Permian rocks.

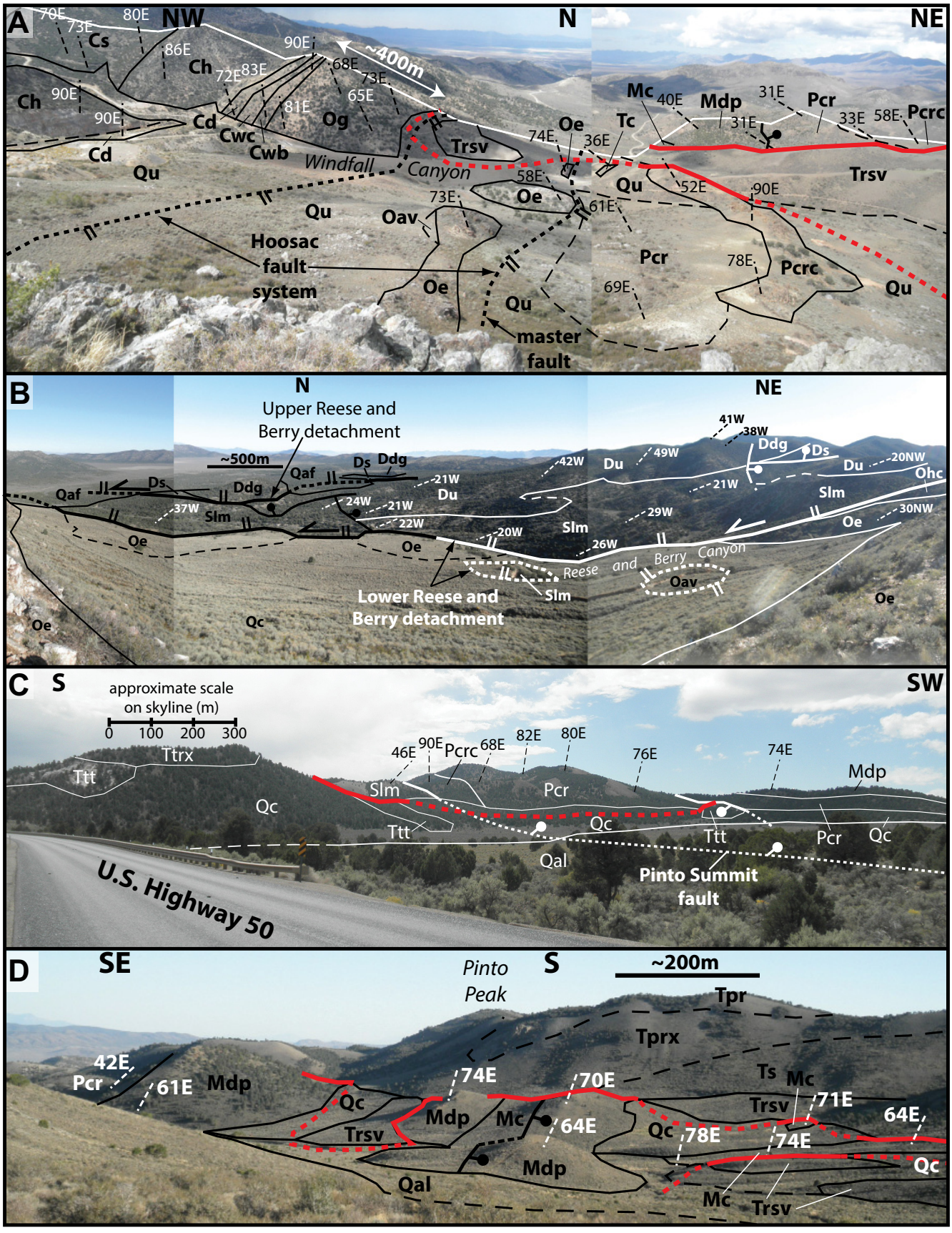
A
NW
N
NE
Cs
Ch
Cd
Cwc
Cwb
Og
Qu
Windfall Canyon
Trsv
Oe
Oav
Hoosac fault system
master fault
Mc
Mdp
Pcr
Pcrc
Tc
~400m
B
N
Upper Reese and Berry detachment
~500m
NE
Qaf
Ds
Ddg
Du
Slm
Oe
Qc
Lower Reese and Berry detachment
Reese and Berry Canyon
Oav
Ohc
C
S
SW
approximate scale on skyline (m)
0 100 200 300
Ttrx
Ttt
Qc
Slm
Pcr
Pcrc
Mdp
Qal
U.S. Highway 50
Pinto Summit fault
D
SE
S
Pinto Peak
~200m
Tpr
Tprx
Ts
Mc
Trsv
Mdp
Qc
Qal

Figure 7.

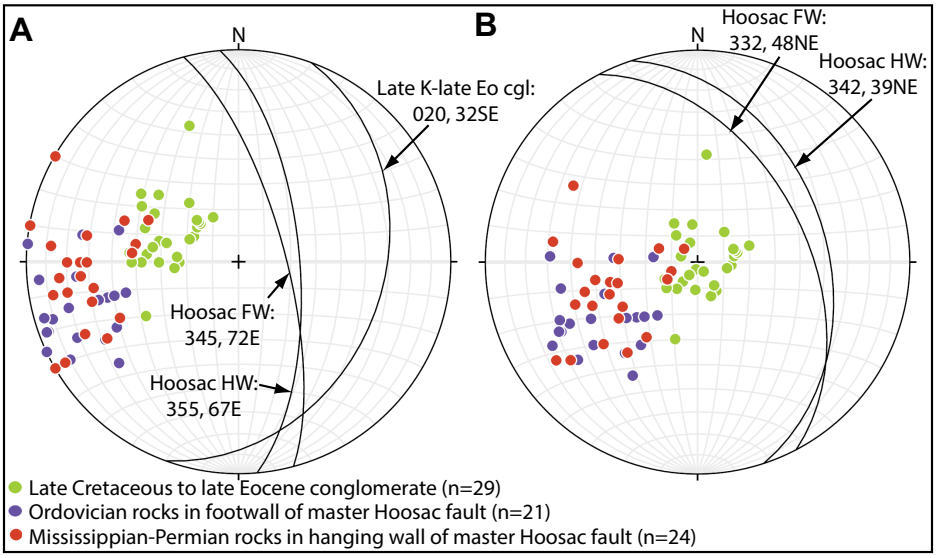

Figure 8. Equal-area stereonet plots (generated using Stereonet 8; Allmendinger et al., 2011). (A) Poles to planes of bedding of Ordovician rocks in footwall (FW) of master Hoosac fault (purple), Mississippian–Permian rocks in its hanging wall (HW; red), and overlapping Late Cretaceous to late Eocene conglomerate (Late K–late Eo cgl; green). Great circles show median bedding orientation for all measurements. Plot defines angular unconformity with ~40° of differential tilt between Paleozoic rocks and conglomerate. (B) Same data as in A, but rotated so average bedding of Late Cretaceous to late Eocene conglomerate (020°, 32°SE) is restored to horizontal. Great circles for median bedding of rocks in footwall and hanging wall of Hoosac fault are an approximation for original eastern limb dip of Eureka culmination at this locality.

Hoosac Mountain 20°–30° to the east (Plate 1; Fig. 8). This brackets the maximum motion age on the Pinto Summit fault as ca. 72 Ma, the maximum deposition age of the conglomerate. In addition, because the conglomerate overlaps the Hoosac fault system, but was likely tilted eastward by motion on the Pinto Summit fault, this indicates that the Hoosac fault system predates the Pinto Summit fault (Plates 1–3).

In summary, normal faults in the map area can be divided into two distinct sets, both of which predate late Eocene (ca. 37 Ma) volcanism: (1) an older set consisting of the down-to-the-east Hoosac fault system and down-to-the-west Reese and Berry detachment system, which have low (≤20°) cutoff angles to bedding, and offset magnitudes between ~2 and 5 km; and (2) a younger set consisting of high-dip-angle (60°–70°), down-to-the-west normal faults with offset magnitudes between 2 and 4.5 km, including the Dugout Tunnel, Lookout Mountain, and Pinto Summit faults. Faults of set 1 are cut and tilted by faults of set 2, and faults of set 2 cut a Late Cretaceous (ca. 86 Ma) contact aureole and tilt conglomerate that has a Late Cretaceous (ca.72 Ma) maximum deposition age. Motion on faults of set 2 was accompanied by as much as to ~20°–30° of eastward tilting.

Geometry of the Late Eocene Subvolcanic Unconformity

The map patterns of late Eocene volcanic rocks, as well as the map-scale geometry of the subvolcanic unconformity, indicate that only minor (≤10°) tilting or vertical throw on normal faults has taken place in most of the map area since the late Eocene. For example, the ~9 km^2 Pinto Peak rhyolite dome is rimmed with volcanic breccia and pyroclastic deposits that exhibit subhorizontal map patterns (Plate 1; Fig. 7D). Volcaniclastic deposits associated with the Ratto Springs dacite have a general ~10°SE dip, which may partly reflect deposition on paleotopography, but are capped by conglomerate and gravel that exhibit subhorizontal basal contacts and yield variable strike directions and dip angles typically ≤7° (Plate 1).

The late Eocene unconformity is exposed in three or more localities on each cross section, distributed across the eastern two-thirds of the map area (Plates 1–3). The cross sections illustrate that the late Eocene erosion surface mimics the modern erosion surface, and is not tilted at a regional scale (Plate 3). Notably, the topographic lows of several prominent canyons incised into Paleozoic bedrock contain exposures of late Eocene volcanic rocks (Plate 1), indicating that these canyons must have been incised by the late Eocene.

Geometry and Stratigraphic Level of the Early Cretaceous Unconformity

The Early Cretaceous NCF is only preserved in the northeast corner of the map area, in a series of exposures that unconformably overlie the Mississippian Diamond Peak Formation and Pennsylvanian Ely Limestone (Plate 1). However, the 5-km-long, semicontinuous exposure that contains the type section of the NCF is located 1–5 km north of the map area (Figs. 2 and 10), where the formation unconformably overlies the Mississippian Diamond Peak Formation, Pennsylvanian Ely Limestone, and Permian Carbon Ridge Formation (Nolan et al., 1971, 1974). Nolan et al. (1971) also mapped the NCF unconformably overlying the Mississippian Diamond Peak Formation and Permian Carbon Ridge Formation 1–4 km north of the map area, at and south of the town of Eureka (Fig. 2).

Within our map area, Nolan et al. (1974) mapped several isolated exposures of conglomerate and other lithologies that unconformably overlie rocks between Ordovician and Permian in age as the NCF. We have reexamined all of these exposures, and we map them as a variety of different rock units, including Permian conglomerate, Late Cretaceous to late Eocene conglomerate, sedimentary rocks associated with late Eocene volcanism, and Quaternary colluvium. Figure SM6 in the Supplemental File (see footnote 1) shows a side by side comparison of our mapping and the mapping of Nolan et al. (1974), as well as field photographs of outcrops, for areas of key importance where we have disagreed with their mapping of the NCF. These areas include: (1) the axis of the Sentinel Mountain syncline (Fig. SM6A in the Supplemental File [see footnote 1]), where we map unconsolidated and locally cemented angular limestone cobbles and boulders that overlie Devonian rocks as Quaternary colluvium; (2) areas in the footwall of the Pinto Summit fault (Fig. SM6B in the Supplemental File [see footnote 1]) where we map pebble conglomerate with a white, tuffaceous matrix that overlies Silurian rocks as conglomerate associated spatially and temporally with late Eocene volcanism, similar to other synvolcanic conglomerate mapped near Pinto Summit; and (3) on Hoosac Mountain (Fig. SM6C in the Supplemental File [see footnote 1]), where red matrix, limestone-clast pebble conglomerate that overlies Ordovician rocks in the footwall of the Hoosac fault system, and Mississippian and Permian rocks in its hanging wall, yields a Late

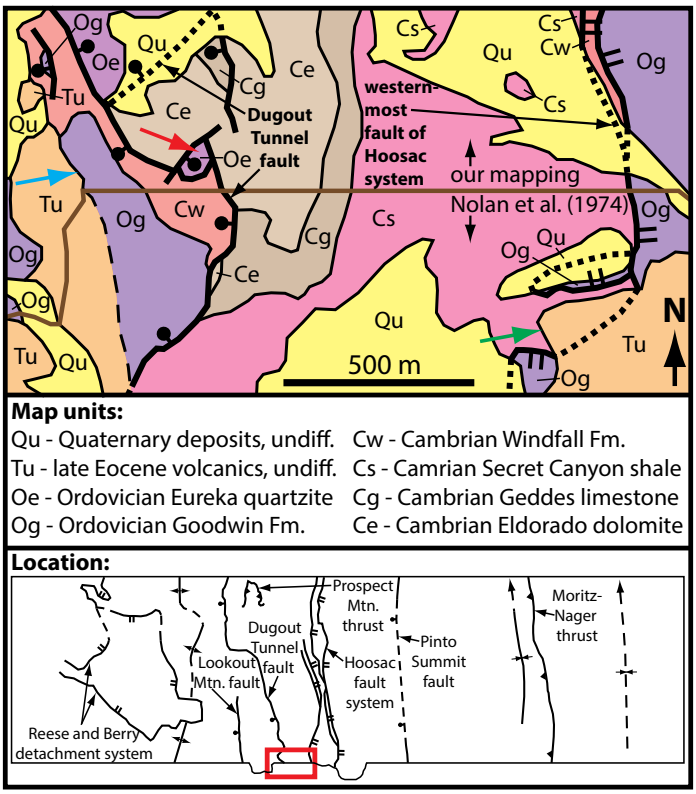

Figure 9. Geologic map of southern part of Secret Canyon (location shown in lower inset and in Fig. 2), showing field relationships of late Eocene unconformity on either side of Dugout Tunnel fault. Unconformity is on Cambrian Secret Canyon Shale in footwall (green arrow) and on Ordovician Goodwin Formation in hanging wall (blue arrow). Units as high in the section as Eureka Quartzite are locally preserved in hanging wall (red arrow).

Cretaceous (ca. 72 Ma) youngest detrital zircon population, and is therefore a distinctly younger rock unit than the NCF.

Our new mapping and geochronology data refute the original interpretation of Nolan et al. (1974) that the NCF was deposited on strata as old as Ordovician, Silurian, and Devonian, and therefore have fundamental implications for the map-scale geometry and basal structural relief of the Early Cretaceous unconformity. The ages of subcrop units observed beneath NCF exposures in the northeast part of our map area (Plate 1), in the type exposure (Fig. 10) (Nolan et al., 1971, 1974), and at and south of the town of Eureka (Fig. 2) (Nolan et al., 1971, 1974), show that stratigraphic levels below the Mississippian Diamond Peak Formation were not breached by the Early Cretaceous. This indicates that the NCF was deposited on a substrate of Mississippian to Permian rocks that had a maximum regional structural relief of ~1.5 km, estimated using stratigraphic thicknesses in Figure 3.

The low structural relief of the Early Cretaceous unconformity also has important implications for the maximum motion age of the Pinto Summit fault and Hoosac fault system, which Nolan et al. (1974) originally mapped as being overlapped by the Early Cretaceous unconformity. Subcrop relationships defined by our new mapping show that the NCF overlies similar stratigraphic levels on either side of the Pinto Summit fault, indicating that it cuts the Early Cretaceous unconformity (Plate 3). Our mapping and geochronology data show that the NCF is not preserved in the footwall of the Hoosac fault system, which suggests that this fault system also cuts the Early Cretaceous unconformity.

EUREKA CULMINATION

The cross sections on the bottom row of Plate 3 were retrodeformed for extensional deformation, which was accomplished by: (1) matching line lengths and angles between the deformed and restored cross sections (e.g., Dahlstrom, 1969); (2) restoring the displacements of matching hanging-wall and footwall cutoffs across all normal faults; and (3) retrodeformation of ~25° of eastward tilting in the hanging wall of the Pinto Summit fault, based on the dip of the Late Cretaceous to late Eocene conglomerate on Hoosac Mountain. Details on additional constraints used in retrodeforming extension are annotated in footnotes in Plate 3. Comparison of deformed and restored lengths reveals similar extension magnitudes for all three cross sections, with a total range of 7.4–8.1 km (~45%–50% extension).

Retrodeformation of extension reveals a similar preextensional deformation geometry on all three cross sections, defined by an upright anticline with a wavelength between 19 and 21 km and an amplitude between 4.3 and 5.0 km, which is here named the Eureka culmination. The existence of this regional structural high is independently corroborated by Paleogene subcrop and erosion patterns. In Long (2012), a paleogeologic map of the Sevier hinterland was presented that showed the distribution of Neoproterozoic to Triassic rocks exposed beneath the regional Paleogene, subvolcanic unconformity, and illustrated the approximate map patterns of regional-scale, pre-unconformity structures. Figure 11 shows a Paleogene subcrop map of the Eureka region (modified from Long, 2012) that reveals the approximate map patterns of several north-trending, erosionally beveled, pre-Paleogene folds, with erosion levels typically in Mississippian to Triassic rocks. However, the Eureka culmination exhibits erosion levels as much as 4 km deeper than the folds in the surrounding ranges, and can be traced along strike for ~100 km, from the northern Pancake Range, where it exhibits Ordovician subcrop levels, through the study area, where subcrop levels are as deep as Cambrian, and into Diamond Valley, on the basis of Devonian and Mississippian subcrop levels observed in drill holes. In the study area deep subcrop levels represent a combination of erosional exhumation of the Eureka culmination during and after its construction, and tectonic exhumation by pre–late Eocene normal faulting.

Structural Model

In regions that have undergone superposed contractional and extensional tectonism, one of the largest uncertainties in restoring and quantifying deformation is how to differentiate between the effects of tilting and folding associated with motion on normal faults versus motion on thrust faults. In our cross sections, this equates to uncertainty in how to model the relationships of kink surfaces to the geometries of specific structures at depth, because folding

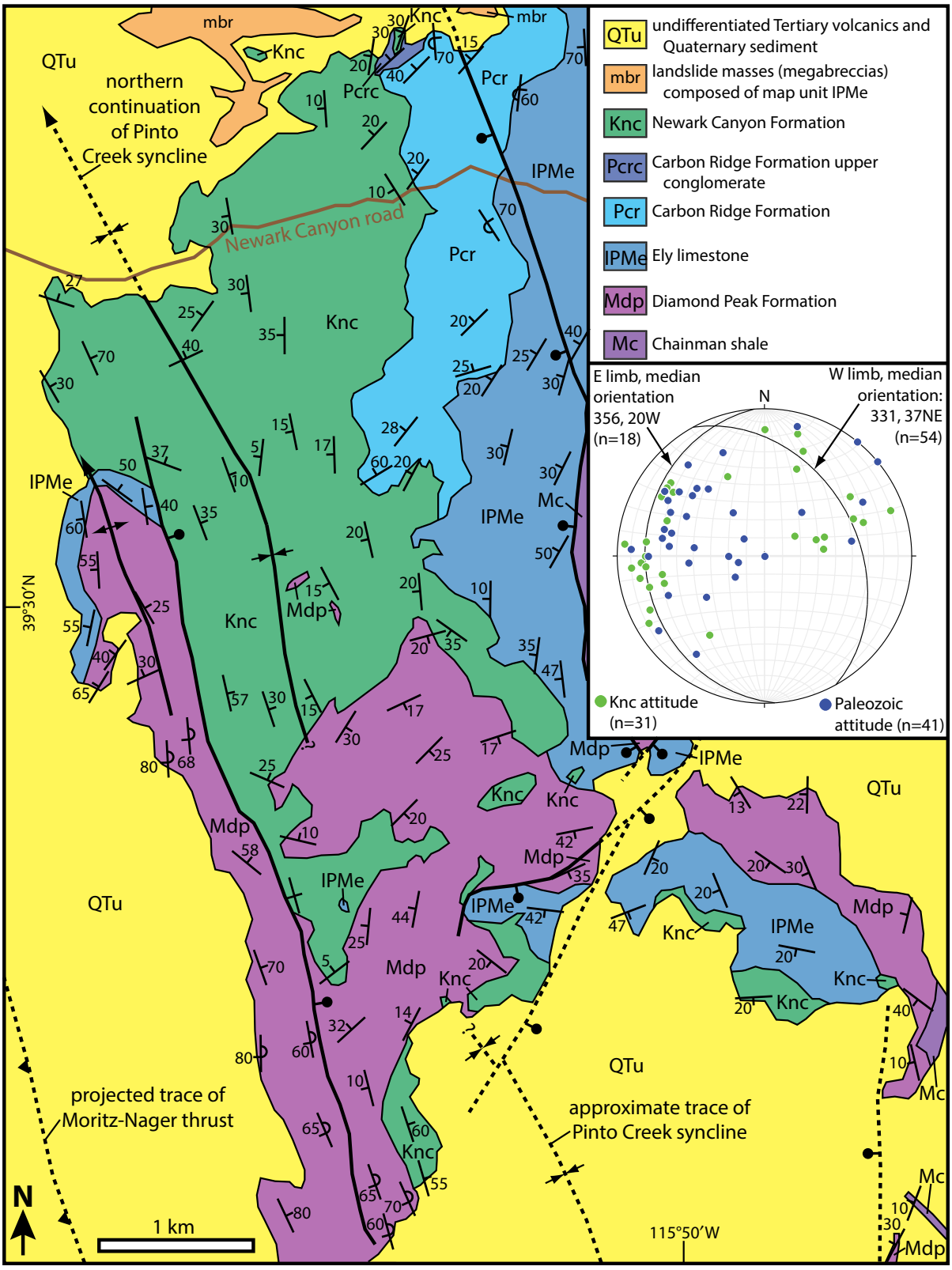

Figure 10. Geologic map of part of southern Diamond Mountains, adjoining north edge of Plate 1 (location shown in Fig. 2), simplified from Nolan et al. (1971, 1974), illustrating map pattern of exposure that contains type section of Newark Canyon Formation (type section is along Newark Canyon road). Early Cretaceous unconformity is on map units Mdp, IPMe, Pcr, and Pcrc. Stereonet plot (equal-area, generated using Stereonet 8; Allmendinger et al., 2011) shows poles to planes of bedding for Paleozoic and Cretaceous rocks, and median limb orientations of Pinto Creek syncline, based on all Paleozoic–Cretaceous attitudes in each limb.

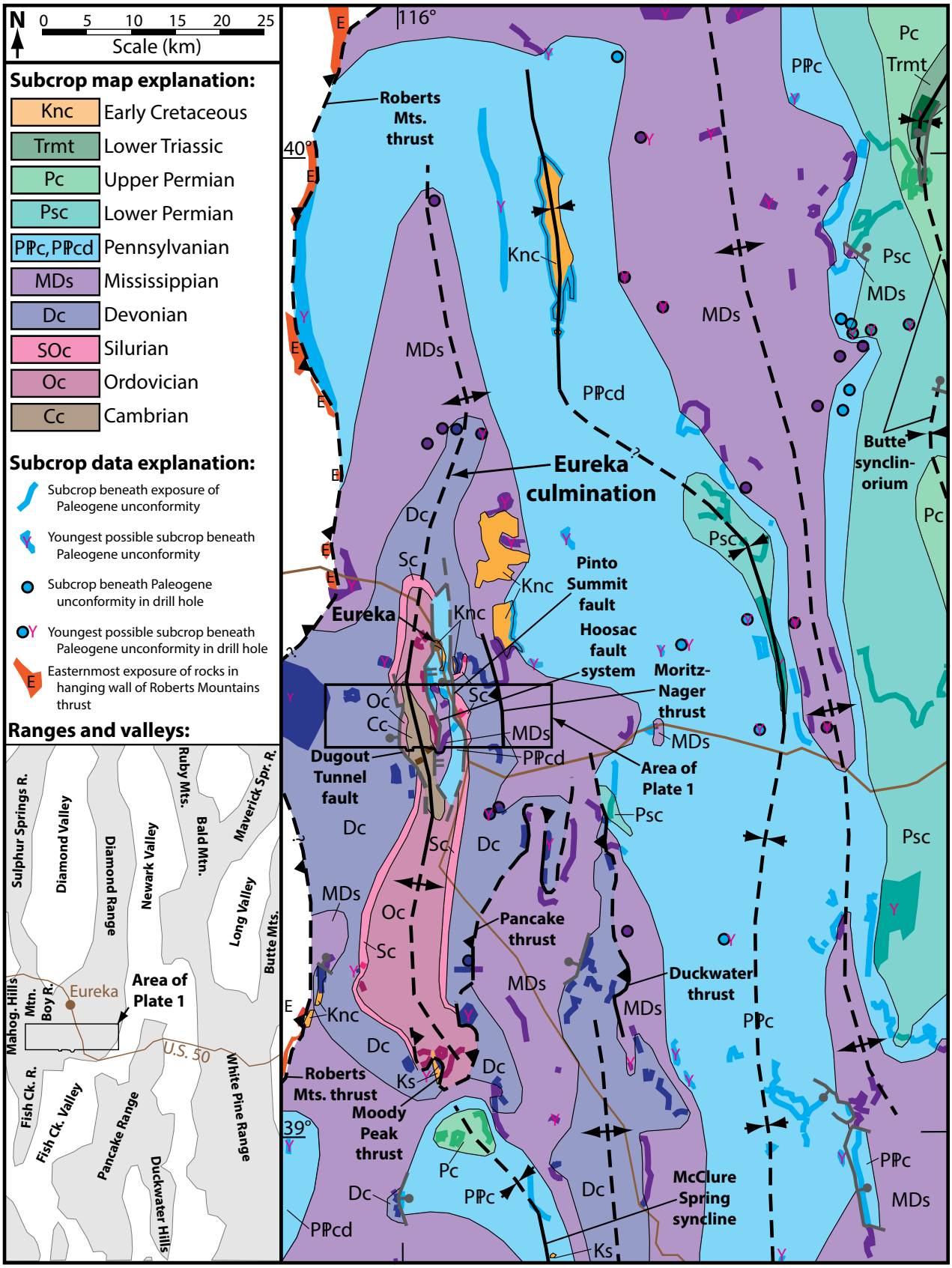

Figure 11. Paleogene subcrop map of Eureka region (modified from Long, 2012), showing subcrop patterns of regional-scale, erosionally beveled, pre-Paleogene folds (including Eureka culmination), Newark Canyon Formation exposures, and pre–late Eocene normal faults in study area.

can be attributed to changes in the geometry of nonplanar normal faults (e.g., Hamblin, 1965; Groshong, 1989; Dula, 1991; Xiao and Suppe, 1992) or thrust faults (e.g., Boyer and Elliott, 1982; Suppe, 1983; Mitra, 1990). Therefore, determining how to fill the space in the cross sections beneath the Moritz-Nager thrust and, more important, beneath the structurally lower, larger offset Ratto Canyon thrust, is the largest uncertainty in the cross sections. This space must be filled with structurally repeated Paleozoic rocks (Plate 3), and many geometric solutions are possible. Because the uncertainty in projection of kink surfaces and corresponding dip domains propagates with depth, as more structures are crossed, a simplified structural model for contractional deformation in the study area is presented here (Fig. 12), rather than attempting to balance fault offsets and cutoff angles for contractional structures on individual cross sections.

First-order observations that must be satisfied in the structural model include the following: (1) the Eureka culmination has a wavelength of ~20 km, an amplitude of ~4.5 km, and preextensional average limb dips between 25° and 35°; (2) rocks as deep as the Cambrian Prospect Mountain Quartzite are exposed in the hanging wall of the Ratto Canyon thrust, indicating the highest permissible stratigraphic position for the regional basal dècollemont; (3) the Silurian Lone Mountain Dolomite is in the footwall of the Ratto Canyon thrust under the culmination crest; and (4) older-over-younger relationships are not observed in the footwall of the Moritz-Nager thrust, where strata as deep as the Devonian Oxyoke Canyon Sandstone are exposed (Plate 1); therefore, all rocks exposed in the Diamond Mountains are interpreted to be in the hanging wall of the Ratto Canyon thrust, which cannot have ramped upsection through more than 300 m of footwall stratigraphy between here and its interception recorded in drill holes ~10 km to the west.

The simplest structural model that explains these observations is that the Eureka culmination represents a fault-bend fold (e.g., Suppe, 1983) constructed by eastward motion of the Ratto Canyon thrust sheet over a footwall ramp that cuts from the Cambrian Prospect Mountain Quartzite to the Silurian Lone Mountain Dolomite, and then forms a footwall flat within the Silurian section toward the east (Figs. 12A, 12B). The Prospect Mountain thrust is shown using the Ratto Canyon thrust surface along and west of its footwall ramp, and branching upward from the top of the footwall ramp at a ~35° cutoff angle to strata (Figs. 12B–12C). Based on their similar offset sense and magnitude, the relative stratigraphic levels that they deform, and a lack of any surface-breaching thrust faults observed between their traces, the Prospect Mountain and Moritz-Nager thrusts are connected as the same structure at depth (Fig. 12C; Plate 3). The Sentinel Mountain syncline is interpreted as the trailing axis of a fault-bend fold that formed above a footwall ramp on the Moritz-Nager thrust (Fig. 12C).

The 20 km wavelength and 4.5 km amplitude of the Eureka culmination can be reproduced with a 27° footwall ramp angle, which is an approximate average of the dips of the western and eastern limbs, 9 km of displacement on the Ratto Canyon thrust, and an additional 1 km of displacement on the Prospect Mountain–Moritz-Nager thrust, for a total of 10 km

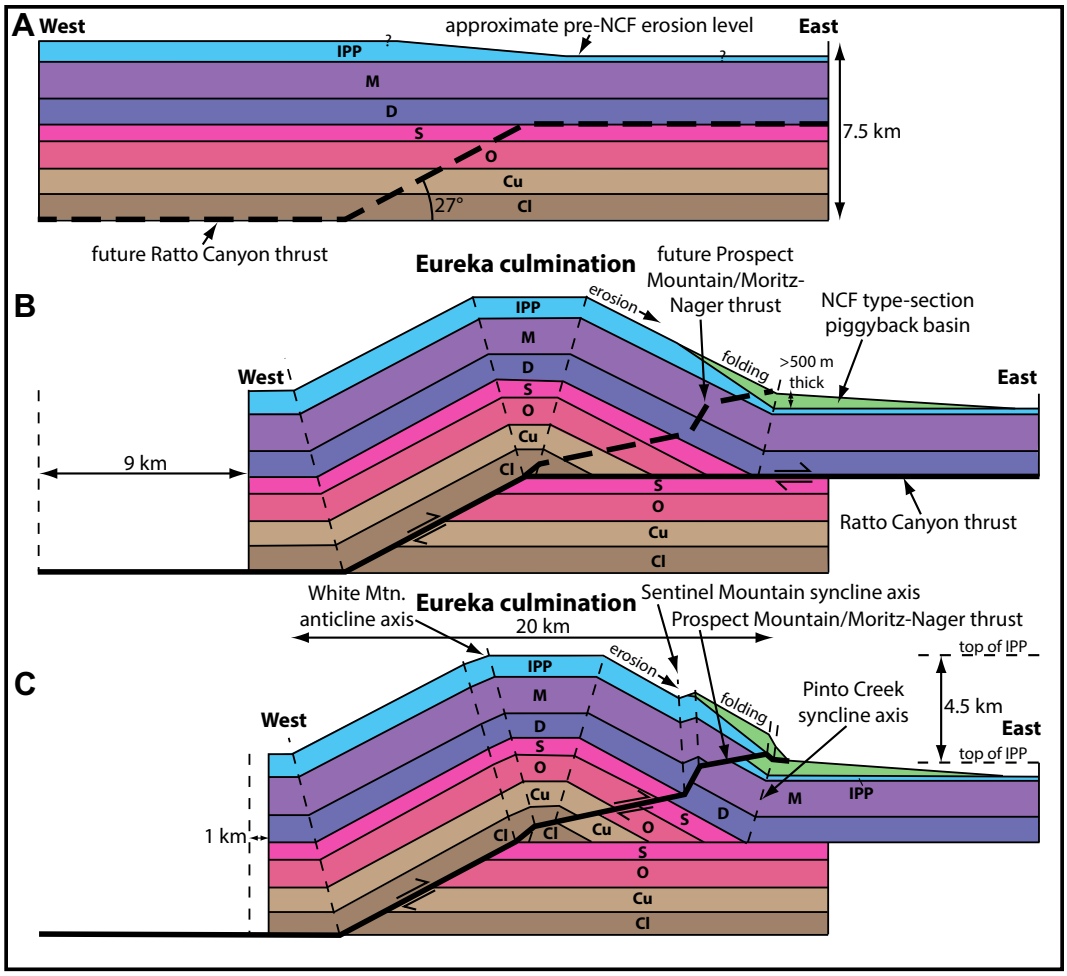

Figure 12. Simplified structural model for central Nevada thrust belt (CNTB) deformation in map area, showing construction of Eureka culmination as a fault-bend fold (abbreviations: Cl—lower Cambrian, Cu—upper Cambrian, O—Ordovician, S—Silurian, D—Devonian, M—Mississippian, IPP—Pennsylvanian and Permian; see Fig. 3). (A) Undeformed geometry. NCF—Newark Canyon Formation. (B) 9 km of eastward motion of Ratto Canyon thrust sheet over footwall ramp that cuts from base of unit Cl to top of unit S, and coeval deposition and folding of Newark Canyon Formation (NCF) in piggyback basin on eastern limb of culmination. (C) 1 km eastward displacement on Prospect Mountain/Moritz-Nager thrust, shown reactivating Ratto Canyon thrust along and west of footwall ramp, and branching from top of footwall ramp.

of horizontal shortening (Fig. 12). Because this is a simplified geometric model, this shortening estimate should be considered approximate.

DISCUSSION

Relationship of Eureka Culmination to NCF Deposition

Fundamental questions remain regarding the timing and geometric relationship of NCF deposition to regional deformation, as demonstrated by the diverse range of scenarios proposed in previous studies (e.g., Nolan et al., 1974; Vandervoort and Schmitt, 1990; Carpenter et al., 1993; Ransom and Hansen, 1993; Taylor et al., 1993). Based on clast composition and detrital zircon provenance data indicating derivation from proximal late Paleozoic subcrop units, Vandervoort and Schmitt (1990) and Druschke et al. (2011) suggested that deposition in the type-NCF basin may have been contemporary with proximal CNTB deformation. However, these studies lack the necessary structural context to relate NCF deposition to motion on specific faults or growth of folds. The revised CNTB structural model presented here provides this context and facilitates interpretation of NCF deposition from the perspective of the regional preextensional deformation geometry. We propose that the NCF type exposure was deposited in a piggyback basin that developed on the eastern limb of the Eureka culmination as it grew (Figs. 12A, 12B). This implies that culmination growth, as well as related motion on the Ratto Canyon thrust at depth, can be indirectly dated as Aptian (ca. 116 Ma; Druschke et al., 2011).

The total preserved across-strike structural relief of the basal NCF unconformity is ~1.5 km; structural relief of the eastern limb of the culmination approached 4.5 km by the end of its construction. This indicates that the NCF was deposited during the early stages of fold growth (Fig. 12B). The most likely sediment source was erosion of the culmination crest, which is compatible with provenance data suggesting derivation from proximal late Paleozoic subcrop units (Vandervoort and Schmitt, 1990; Druschke et al., 2011) and east-directed paleocurrent directions (Vandervoort, 1987). After deposition, the NCF continued to be folded during late-stage growth of the culmination, represented by the northward continuation of the Pinto Creek syncline into the NCF type exposure (Nolan et al., 1971) (Fig. 10), which in our structural model corresponds to the leading axis of the hanging-wall cutoff of the Ratto Canyon thrust sheet (Fig. 12C).

Lateral lithologic variability coupled with a lack of precise deposition age control make regional correlations between isolated NCF exposures tentative (e.g., Vandervoort, 1987; Carpenter et al., 1993). For example, on the basis of biostratigraphy, rocks mapped as NCF in the Fish Creek Range can only be narrowed between Barremian and Albian (Fouch et al., 1979; Hose, 1983), and rocks mapped as NCF in the Pinon Range and Cortez Mountains are broadly bracketed as Early to Late Cretaceous (Smith and Ketner, 1976; Fouch et al., 1979). In addition, in the Pancake Range and northern Diamond Mountains, rocks mapped as NCF (Stewart and Carlson, 1978; Kleinhampl and Ziony, 1985) have been alternatively interpreted as Permian (Larson and Riva, 1963; Perry and Dixon, 1993), with no published biostratigraphic age control. The Aptian deposition age defined in the type exposure (Druschke et al., 2011) provides the only precise age control of any NCF exposure to date. Therefore, although it is possible that other exposures mapped as NCF along strike were deposited in a regional belt of Early Cretaceous contractional deformation, the precise age control and detailed structural context necessary to convincingly demonstrate this are currently lacking, and indicate the need for additional mapping and geochronology.

Implications for Out-Of-Sequence Deformation in the Sevier Hinterland

The timing of initiation of deformation in the Sevier thrust belt in Utah is a subject of long-standing debate (e.g., Armstrong, 1968; Jordan, 1981; Wiltschko and Dorr, 1983; Heller et al., 1986; DeCelles, 2004). The onset of subsidence in the Sevier foreland basin, which is attributed to loading from crustal thickening in the Sevier thrust belt, occurred by at least ca. 125 Ma (Aptian-Barremian boundary) (Jordan, 1981), and has been argued to be as old as ca. 145 Ma (latest Jurassic) (DeCelles, 2004; DeCelles and Coogan, 2006). Therefore, Aptian (ca. 116 Ma) growth of the Eureka culmination postdated migration of the Sevier thrust front into Utah by at least ~10 m.y., and possibly as much as ~30 m.y., defining out-of-sequence hinterland deformation.

Using a regional balanced cross section, DeCelles and Coogan (2006) documented 220 km of total shortening in the type-Sevier thrust belt in western Utah, at the approximate latitude of Eureka (Fig. 1). More than half (117 km) of this total shortening was accommodated by emplacement of the Canyon Range thrust sheet, which may have initiated as early as the latest Jurassic (ca. 145 Ma), and lasted until ca. 110 Ma, when the deformation front migrated forward to the Pavant thrust sheet (Fig. 13) (DeCelles and Coogan, 2006). Therefore, construction of the Eureka culmination in the hinterland was coeval with late-stage emplacement of the Canyon Range thrust sheet. This thick, areally extensive thrust sheet is exposed across all of westernmost Utah and eastern Nevada at this latitude, and was translated a total of 140 km eastward during Sevier orogenesis; this is attributed to high rheological competence as a result of carrying a ~7-km-thick section of Neoproterozoic–early Cambrian quartzite (DeCelles, 2004). The dimensions of the Canyon Range thrust sheet, which approach 250 km across strike and 700 km along strike (estimate includes the correlative Paris-Willard thrust to the north; e.g., Armstrong, 1968), rank among the largest recorded thrust sheets in foreland thrust belts (Hatcher and Hooper, 1992; Hatcher, 2004), and may approach a critical mechanical upper bound for this tectonic setting.

Numerical and analog models predict that the critical taper angle of an orogenic wedge that must be achieved to allow forward propagation is governed by the relative magnitudes of

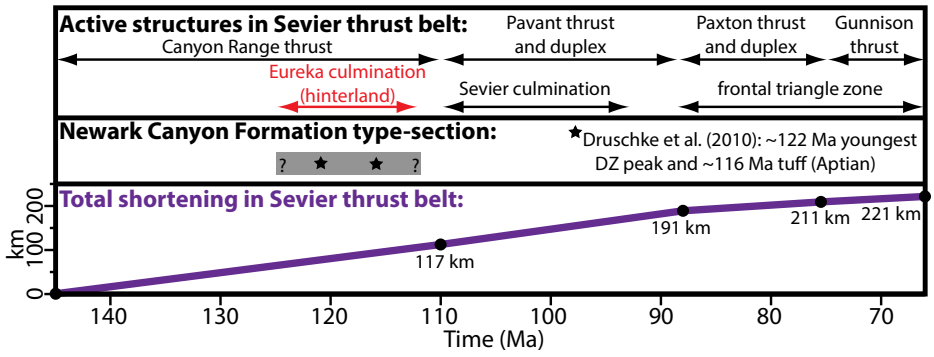

Figure 13. Graph showing timing of active structures and cumulative shortening magnitudes reported for type-Sevier thrust belt (DeCelles and Coogan, 2006). Approximate Aptian deposition age range (125–112 Ma) is shown for Newark Canyon Formation. DZ—detrital zircon.

the frictional strength of the basal dècollemont and the compressive strength of the rocks in the orogenic wedge (e.g., Chapple, 1978; Davis et al., 1983; Dahlen et al., 1984; Dahlen, 1990). Assuming that the strength of rocks within the Canyon Range thrust sheet did not change appreciably after accretion into the orogenic wedge, a decrease in basal frictional strength would be necessary for continued eastward translation. This could be accommodated through several different mechanisms, including progressive strain weakening of fault zone rocks, and/or an increase in pore pressure. An additional mechanism would be to decrease frictional strength by shortening the length of the basal dècollemont. This was undoubtedly accomplished through erosional beveling at the thrust front during translation (e.g., DeCelles, 1994), but could also have been assisted through internal shortening of the thrust sheet. The ~10 km of hinterland shortening at Eureka could represent internal shortening of the Canyon Range thrust sheet during emplacement to promote further eastward translation. Because it was located ~180–200 km west of the Canyon Range thrust front (preextensional map distance estimated from McQuarrie and Wernicke, 2005), construction of the Eureka culmination may not have appreciably increased the overall surface slope angle of the orogenic wedge. However, instead of building taper, perhaps this hinterland deformation acted as a mechanism to decrease the overall frictional coupling of the basal dècollemont to promote forward propagation.

Studies focused on the kinematic development of the frontal Sevier thrust belt in Utah have revealed the importance of out-of-sequence growth of structural culminations in the internal parts of the thrust belt as a mechanism to drive propagation of frontal thrust sheets (DeCelles, 1994, 2004; DeCelles and Coogan, 2006). At the latitude of our study area, this included growth of the Sevier culmination, a duplex system in western Utah composed of basement thrust sheets that folds and structurally elevates the Canyon Range thrust sheet (Allmendinger et al., 1986; DeCelles et al., 1995), and growth of duplexes further to the foreland that structurally elevate the Canyon Range and Pavant thrust sheets (DeCelles and Coogan, 2006). Our study demonstrates that, although more local in scale, similar processes were occurring earlier in the Sevier shortening history in the distal portions of the hinterland.

CONCLUSIONS

New mapping and balanced cross sections redefine the first-order structures and deformation geometry of the CNTB at the latitude of Eureka. Retrodeformation of extension defines the Eureka culmination, a north-striking anticline with a 20 km wavelength, a 4.5 km amplitude, and limb dips of 25°–35°, which is corroborated by deep Paleogene erosion levels that can be traced for ~100 km along strike. A Cambrian over Silurian relationship observed in drill holes under the culmination crest defines the blind Ratto Canyon thrust. The culmination is interpreted as a fault-bend fold that formed from translation of the Ratto Canyon thrust sheet ~9 km eastward over a footwall ramp at depth.

The Early Cretaceous (Aptian) type-NCF section was deposited in a piggyback basin on the eastern limb of the Eureka culmination as it grew. Aptian hinterland deformation postdated migration of the Sevier thrust front into Utah by ~10–30 m.y., and was coeval with late-stage emplacement of the orogen-scale Canyon Range thrust sheet. Growth of the Eureka culmination could represent internal shortening of the Canyon Range thrust sheet, which acted as a mechanism to promote further eastward translation.

ACKNOWLEDGMENTS

This work was funded by grants from the U.S. Geological Survey STATEMAP program and from Timberline Resources Corporation (Paul Dircksen, CEO). The $^{40}Ar/^{39}Ar$ ages were determined at the New Mexico Geochronology Research Laboratory (New Mexico Institute of Mining and Technology) under the guidance of Bill McIntosh, Matt Heizler, and Lisa Peters. U-Pb zircon data were acquired at the (U-Th)/He Geo- and Thermochronometry Lab at the University of Texas at Austin with guidance from Daniel Stockli. We thank Jennifer Mauldin and Irene Seelye of the Nevada Bureau of Mines and Geology cartography team, and Mitch Casteel, Bob Thomas, Peter Rugowski, Russell DiFiori, and Lucia Patterson of the Timberline Resources Corporation Eureka exploration team. Comments from three anonymous reviewers and associate editor Terry Pavlis significantly improved this manuscript.

REFERENCES CITED

Allmendinger, R.W., 1992, Fold and thrust tectonics of the western United States exclusive of the accreted terranes, *in* Burchfiel, B.C., et al., eds., The Cordilleran orogen: Conterminous U.S.: Boulder, Colorado, Geological Society of America, Geology of North America, v. G-3, p. 583–607.

Allmendinger, R.W., and Jordan, T.E., 1981, Mesozoic evolution, hinterland of the Sevier orogenic belt: Geology, v. 9, p. 308–313, doi:10.1130/0091-7613(1981)9<308:MEHOTS>2.0.CO;2.

Allmendinger, R.W., Farmer, H., Hauser, E., Sharp, J., Von Tish, D., Oliver, J., and Kaufman, S., 1986, Phanerozoic tectonics of the Basin and Range–Colorado Plateau transition from COCORP data and geologic data: A review, *in* Barazangi, M., and Brown, L., eds., Reflection seismology: The continental crust: American Geophysical Union Geodynamics Series Volume 14, p. 257–267.

Allmendinger, R.W., Cardozo, N., and Fisher, D., 2011, Structural geology algorithms: Vectors and tensors in structural geology: New York, Cambridge University Press, 304 p.

Armstrong, P.A., and Bartley, J.M., 1993, Displacement and deformation associated with a lateral thrust termination, southern Golden Gate Range, southern Nevada, U.S.A: Journal of Structural Geology, v. 15, p. 721–735, doi:10.1016/0191-8141(93)90058-I.

Armstrong, R.L., 1968, Sevier orogenic belt in Nevada and Utah: Geological Society of America Bulletin, v. 79, p. 429–458, doi:10.1130/0016-7606(1968)79[429:SOBINA]2.0.CO;2.

Armstrong, R.L., 1972, Low-angle (denudation) faults, hinterland of the Sevier orogenic belt, eastern Nevada and western Utah: Geological Society of America Bulletin, v. 83, p. 1729–1754, doi:10.1130/0016-7606(1972)83[1729:LDFHOT]2.0.CO;2.

Armstrong, R.L., and Ward, P., 1991, Evolving geographic patterns of Cenozoic magmatism in the North American Cordillera: The temporal and spatial association of magmatism and metamorphic core complexes: Journal of Geophysical Research, v. 96, p. 13,201–13,224, doi:10.1029/91JB00412.

Bartley, J.M., and Gleason, G.C., 1990, Tertiary normal faults superimposed on Mesozoic thrusts, Quinn Canyon and Grant Ranges, Nye County, Nevada, *in* Wernicke, B.P., ed., Basin and Range extensional tectonics near the latitude of Las Vegas, Nevada: Geological Society of America Memoir 176, p. 195–212, doi:10.1130/MEM176-p195.

Barton, M.D., 1987, Lithophile-element mineralization associated with Late Cretaceous two-mica granites in the Great Basin: Geology, v. 15, p. 337–340, doi:10.1130/0091-7613(1987)15<337:LMAWLC>2.0.CO;2.

Best, M.G., and Christiansen, E.H., 1991, Limited extension during peak Tertiary volcanism, Great Basin of Nevada and Utah: Journal of Geophysical Research, v. 96, p. 13,509–13,528, doi:10.1029/91JB00244.

Best, M.G., Barr, D.L., Christiansen, E.H., Gromme, S., Deino, A.L., and Tingey, D.G., 2009, The Great Basin Altiplano during the middle Cenozoic ignimbrite flareup: Insights from volcanic rocks: International Geology Review, v. 51, p. 589–633, doi:10.1080/00206810902867690.

Bjerrum, C.J., and Dorsey, R.J., 1995, Tectonic controls on deposition of Middle Jurassic strata in a retroarc foreland basin, Utah-Idaho trough, western interior, United States: Tectonics, v. 14, p. 962–978, doi:10.1029/95TC01448.

Boyer, S.E., and Elliott, D., 1982, Thrust systems: American Association of Petroleum Geologists Bulletin, v. 66, p. 1196–1230.

Brew, D.A., 1961a, Lithologic character of the Diamond Peak Formation (Mississippian) at the type locality, Eureka and White Pine Counties, Nevada: U.S. Geological Survey Professional Paper 424-C, p. C110–C112.

Brew, D.A., 1961b, Relation of Chainman Shale to Bold Bluff thrust fault, southern Diamond Mountains, Eureka and White Pine Counties, Nevada: U.S. Geological Survey Professional Paper 424-C, p. C113–C115.

Brew, D.A., 1971, Mississippian stratigraphy of the Diamond Peak area, Eureka County, Nevada, with a section on the biostratigraphy and age of the Carboniferous formations, by Mackenzie Gordon, Jr.: U.S. Geological Survey Professional Paper 661, 84 p.

Burchfiel, B.C., and Davis, G.A., 1975, Nature and controls of Cordilleran orogenesis, western United States—Extension of an earlier synthesis: American Journal of Science, v. 275A, p. 363–396.

Burchfiel, B.C., Cowan, D.S., and Davis, G.A., 1992, Tectonic overview of the Cordilleran orogen in the western United States, *in* Burchfiel, B.C., et al., eds., The Cordilleran orogen: Conterminous U.S.: Boulder, Colorado, Geological Society of America, Geology of North America, v. G-3, p. 407–480.

Camilleri, P.A., and Chamberlain, K.R., 1997, Mesozoic tectonics and metamorphism in the Pequop Mountains and Wood Hills region, northeast Nevada: Implications for the architecture and evolution of the Sevier orogen: Geological Society of America Bulletin, v. 109, p. 74–94, doi:10.1130/0016-7606(1997)109<0074:MTAMIT>2.3.CO;2.

Carpenter, D.G., Carpenter, J.A., Dobbs, S.W., and Stuart, C.K., 1993, Regional structural synthesis of Eureka fold-and-thrust belt, east-central Nevada, *in* Gillespie, C.W., ed., Structural and stratigraphic relationships of Devonian reservoir rocks, east-central Nevada: Nevada Petroleum Society 1993 Field Conference Guidebook NPS 07, p. 59–72.

Chapple, W.M., 1978, Mechanics of thin-skinned fold and thrust belts: Geological Society of America Bulletin, v. 89, p. 1189–1198, doi:10.1130/0016-7606(1978)89<1189:MOTFB>2.0.CO;2.

Colgan, J.P., and Henry, C.D., 2009, Rapid middle Miocene collapse of the Sevier orogenic plateau in north-central Nevada: International Geology Review, v. 51, p. 920–961, doi:10.1080/00206810903056731.

Coney, P.J., 1978, Mesozoic–Cenozoic Cordilleran plate tectonics, *in* Smith, R.B., and Eaton, G.P., eds., Cenozoic tectonics and regional geophysics of the western Cordillera: Geological Society of America Memoir 152, p. 33–50, doi:10.1130/MEM152-p33.

Coney, P.J., and Harms, T.J., 1984, Cordilleran metamorphic core complexes: Cenozoic extensional relics of Mesozoic compression: Geology, v. 12, p. 550–554, doi:10.1130/0091-7613(1984)12<550:CMCCCE>2.0.CO;2.

Cook, H.E., and Corboy, J.E., 2004, Great Basin Paleozoic carbonate platform: Facies, facies transitions, depositional models, platform architecture, sequence stratigraphy, and predictive mineral host models: U.S. Geological Survey Open-File Report 2004-1078, 129 p.

Cowell, P.F., 1986, Structure and stratigraphy of part of the Northern Fish Creek Range, Eureka County, Nevada [M.S. thesis]: Corvallis, Oregon State University, 96 p.

Crafford, A.E.J., 2007, Geologic map of Nevada: U.S. Geological Survey Data Series 249, 46 p.

Dahlen, F.A., 1990, Critical taper model of fold-and-thrust belts and accretionary wedges: Annual Review of Earth and Planetary Sciences, v. 18, p. 55–99, doi:10.1146/annurev.ea.18.050190.000415.

Dahlen, F.A., Suppe, J., and Davis, D.M., 1984, Mechanics of fold-and-thrust belts and accretionary wedges: cohesive Coulomb theory: Journal of Geophysical Research, v. 89, p. 10,087–10,101, doi:10.1029/JB089iB12p10087.

Dahlstrom, C.D.A., 1969, Balanced cross-sections: Canadian Journal of Earth Sciences, v. 6, p. 743–757, doi:10.1139/e69-069.

Davis, D., Suppe, J., and Dahlen, F.A., 1983, Mechanics of fold-and-thrust belts and accretionary wedges: Journal of Geophysical Research, v. 88, p. 1153–1172, doi:10.1029/JB088iB02p01153.

DeCelles, P.G., 1994, Late Cretaceous–Paleocene synorogenic sedimentation and kinematic history of the Sevier thrust belt, northeast Utah and southwest Wyoming: Geological Society of America Bulletin, v. 106, p. 32–56, doi:10.1130/0016-7606(1994)106<0032:LCPSSA>2.3.CO;2.

DeCelles, P.G., 2004, Late Jurassic to Eocene evolution of the Cordilleran thrust belt and foreland basin system, western U.S.A: American Journal of Science, v. 304, p. 105–168, doi:10.2475/ajs.304.2.105.

DeCelles, P.G., and Coogan, J.C., 2006, Regional structure and kinematic history of the Sevier fold-and-thrust belt, central Utah: Geological Society of America Bulletin, v. 118, p. 841–864, doi:10.1130/B25759.1.

DeCelles, P.G., Lawton, T.F., and Mitra, G., 1995, Thrust timing, growth of structural culminations, and synorogenic sedimentation in the type area of the Sevier orogenic belt, central Utah: Geology, v. 23, p. 699–702, doi:10.1130/0091-7613(1995)023<0699:TTGOSC>2.3.CO;2.

Dickinson, W.R., 1977, Paleozoic plate tectonics and the evolution of the Cordilleran continental margin, *in* Stewart, J.H., et al., eds., Paleozoic paleogeography of the western United States, Volume 1: Los Angeles, Pacific Section, SEPM (Society of Economic Paleontologists and Mineralogists), p. 137–156.

Dickinson, W.R., 2002, The Basin and Range Province as a composite extensional domain: International Geology Review, v. 44, p. 1–38, doi:10.2747/0020-6814.44.1.1.

Dickinson, W.R., 2004, Evolution of the North American Cordillera: Annual Review of Earth and Planetary Sciences, v. 32, p. 13–45, doi:10.1146/annurev.earth.32.101802.120257.

Dickinson, W.R., 2006, Geotectonic evolution of the Great Basin: Geosphere, v. 2, p. 353–368, doi:10.1130/GES00054.1.

Dickinson, W.R., and Gehrels, G.E., 2009, U-Pb ages of detrital zircons in Jurassic eolian and associated sandstones of the Colorado Plateau: Evidence for transcontinental dispersal and intraregional recycling of sediment: Geological Society of America Bulletin, v. 121, p. 408–433, doi:10.1130/B26406.1.

Druschke, P., Hanson, A.D., Wells, M.L., Rasbury, T., Stockli, D.F., and Gehrels, G., 2009a, Synconvergent surface-breaking normal faults of Late Cretaceous age within the Sevier hinterland, east-central Nevada: Geology, v. 37, p. 447–450, doi:10.1130/G25546A.1.

Druschke, P., Hanson, A.D., and Wells, M.L., 2009b, Structural, stratigraphic, and geochronologic evidence for extension predating Paleogene volcanism in the Sevier hinterland, east-central Nevada: International Geology Review, v. 51, p. 743–775, doi:10.1080/00206810902917941.

Druschke, P., Hanson, A.D., Wells, M.L., Gehrels, G.E., and Stockli, D., 2011, Paleogeographic isolation of the Cretaceous to Eocene Sevier hinterland, east-central Nevada: Insights from U-Pb and (U-Th)/He detrital zircon ages of hinterland strata: Geological Society of America Bulletin, v. 123, p. 1141–1160, doi:10.1130/B30029.1.

Dula, W.F., 1991, Geometric models of listric normal faulting and rollover folds: American Association of Petroleum Geologists Bulletin, v. 75, p. 1609–1625.

Fouch, T.D., Hanley, J.M., and Forester, R.M., 1979, Preliminary correlation of Cretaceous and Paleogene lacustrine and related nonmarine sedimentary and volcanic rocks in parts of the Great Basin of Nevada and Utah, *in* Newman, G.W., and Goode, H.D., eds., Basin and Range Symposium and Great Basin field conference: Rocky Mountain Association of Petroleum Geologists and Utah Geological Association, p. 305–312.

French, D.E., 1993, Thrust faults in the southern Diamond Mountains, Eureka and White Pine counties, Nevada, *in* Gillespie, C.W., ed., Structural and stratigraphic relationships of Devonian reservoir rocks, east-central Nevada: Nevada Petroleum Society 1993 Field Conference Guidebook NPS 07, p. 105–114.

Gans, P.B., and Miller, E.L., 1983, Style of mid-Tertiary extension in east-central Nevada, *in* Gurgel, K.D., ed., Geologic excursions in the overthrust belt and metamorphic core complexes of the intermountain region: Utah Geological and Mineral Survey Special Studies Volume 59, p. 107–160.

Greene, D.C., 2014, The Confusion Range, west-central Utah: Fold-thrust deformation and a western Utah thrust belt in the Sevier hinterland: Geosphere, v. 10, p. 148–169, doi:10.1130/GES00972.1.

Groshong, R.J., Jr., 1989, Half-graben structures: Balanced models of extensional fault-bend folds: Geological Society of America Bulletin, v. 101, p. 96–105, doi:10.1130/0016-7606(1989)101<0096:HGSBMO>2.3.CO;2.

Hague, A., 1892, Geology of the Eureka district, Nevada: U.S. Geological Survey Monograph 20, 419 p.

Hamblin, W.K., 1965, Origin of "reverse-drag" on the downthrown side of normal faults: Geological Society of America Bulletin, v. 76, p. 1145–1164, doi:10.1130/0016-7606(1965)76[1145:OORDOT]2.0.CO;2.

Hatcher, R.D., Jr., 2004, Properties of thrusts and upper bounds for the size of thrust sheets, *in* McClay, K.R., ed., Thrust tectonics and hydrocarbon systems: American Association of Petroleum Geologists Memoir 82, p. 18–29.

Hatcher, R.D., Jr., and Hooper, R.J., 1992, Evolution of crystalline thrust sheets in the internal parts of mountain chains, *in* McClay, K.R., ed., Thrust tectonics: New York, Chapman and Hall, p. 217–233.

Heller, P.L., Bowdler, S.S., Chambers, H.P., Coogan, J.C., Hagen, E.S., Shuster, M.W., Winslow, N.S., and Lawton, T.F., 1986, Time of initial thrusting in the Sevier Orogenic belt, Idaho-Wyoming and Utah: Geology, v. 14, p. 388–391, doi:10.1130/0091-7613(1986)14<388:TOITIT>2.0.CO;2.

Henry, C.D., 2008, Ash-flow tuffs and paleovalleys in northeastern Nevada: Implications for Eocene paleogeography and extension in the Sevier hinterland, northern Great Basin: Geosphere, v. 4, p. 1–35, doi:10.1130/GES00122.1.

Hodges, K.V., and Walker, J.D., 1992, Extension in the Cretaceous Sevier orogen, North American Cordillera: Geological Society of America Bulletin, v. 104, p. 560–569, doi:10.1130/0016-7606(1992)104<0560:EITCSO>2.3.CO;2.

Hose, R.K., 1983, Geologic map of the Cockalorum Wash quadrangle, Eureka and Nye counties, Nevada: U.S. Geological Survey Miscellaneous Investigations Series Map I-1410, scale 1:31,680.

Jordan, T.E., 1981, Thrust loads and foreland basin evolution, Cretaceous, western United States: American Association of Petroleum Geologists Bulletin, v. 65, p. 2506–2520.

Kleinhampl, F.J., and Ziony, J.L., 1985, Geology of northern Nye County, Nevada: Nevada Bureau of Mines Bulletin 99A, 171 p.

Kuiper, K.F., Deino, A., Hilgen, F.J., Krijgsman, W., Renne, P.R., and Wijbrans, J.R., 2008, Synchronizing rock clocks of Earth history: Science, v. 320, p. 500–504, doi:10.1126/science.1154339.

Larson, E.R., and Riva, J.F., 1963, Preliminary geologic map and sections of the Diamond Springs quadrangle: Nevada Bureau of Mines and Geology Map 20, scale 1:62,550.

Lisenbee, A.L., 2000, Low-angle extensional faulting, Mahogany Hills–Mountain Boy Range, Eureka County, Nevada: Geological Society of America Abstracts with Programs, v. 32, no. 7, p. A-508.

Lisenbee, A.L., 2001a, Synopsis of the geologic evolution of the Eureka area, Nevada, *in* Miller, M.S., and Walker, J.P., eds., Structure and stratigraphy of the Eureka, Nevada, area: Reno, Nevada Petroleum Society 2001 Fieldtrip Guidebook NPS 16, p. 1–17.

Lisenbee, A.L., 2001b, Structure and stratigraphy of the Eureka area, *in* Miller, M.S., and Walker, J.P., eds., Structure and stratigraphy of the Eureka, Nevada, area: Reno, Nevada Petroleum Society 2001 Fieldtrip Guidebook NPS 16, p. 43–58.

Lisenbee, A.L., Monteleone, S.R., and Saucier, A.E., 1995, The Hoosac thrust and related faults, Eureka region, Nevada, *in* Hansen, M.W., et al., eds., Mississippian source rocks in the Antler basin of Nevada and associated structural and stratigraphic traps: Nevada Petroleum Society 1995 Fieldtrip Guidebook NPS 10, p. 115–121.

Long, S.P., 2012, Magnitudes and spatial patterns of erosional exhumation in the Sevier hinterland, eastern Nevada and western Utah, USA: Insights from a Paleogene paleogeologic map: Geosphere, v. 8, p. 881–901, doi:10.1130/GES00783.1.

Long, S.P., Henry, C.D., Muntean, J.H., Edmondo, G.P., and Thomas, R.D., 2012, Preliminary geologic map of the southern Eureka mining district, Eureka and White Pine Counties, Nevada: Nevada Bureau of Mines and Geology Open-File Report 12-6, scale 1:24,000.

MacNeil, F.S., 1939, Fresh-water invertebrates and land plants of Cretaceous age from Eureka, Nevada: Journal of Paleontology, v. 13, p. 355–360.

Martin, A.J., Wyld, S.J., Wright, J.E., and Bradford, J.H., 2010, The Lower Cretaceous King Lear Formation, northwest Nevada: Implications for Mesozoic orogenesis in the western U.S. Cordillera: Geological Society of America Bulletin, v. 122, p. 537–562, doi:10.1130/B26555.1.

Marvin, R.F., and Cole, J.C., 1978, Radiometric ages: Compilation A, U.S. Geological Survey: Isochron-West, no. 22, p. 3–14.

McGrew, A.J., Peters, M.T., and Wright, J.E., 2000, Thermobarometric constraints on the tectonothermal evolution of the East Humboldt Range metamorphic core complex, Nevada: Geological Society of America Bulletin, v. 112, p. 45–60, doi:10.1130/0016-7606(2000)112<45:TCOTTE>2.0.CO;2.

McIntosh, W.C., Heizler, M., Peters, L., and Esser, R., 2003, $^{40}Ar/^{39}Ar$ geochronology at the New Mexico Bureau of Geology and Mineral Resources: New Mexico Bureau of Geology and Mineral Resources Open-File Report OF-AR-1, 10 p.

McQuarrie, N., and Wernicke, B.P., 2005, An animated tectonic reconstruction of southwestern North America since 36 Ma: Geosphere, v. 1, p. 147–172, doi:10.1130/GES00016.1.

Miller, D.M., and Hoisch, T.D., 1995, Jurassic tectonics of northeastern Nevada and northwestern Utah from the perspective of barometric studies, *in* Miller, D.M., and

Busby, C., eds., Jurassic magmatism and tectonics of the North American Cordillera: Geological Society of America Special Paper 299, p. 267–294, doi:10.1130/SPE299-p267.

Miller, E.L., Gans, P.B., Wright, J.E., and Sutter, J.F., 1988, Metamorphic history of the east-central Basin and Range province: Tectonic setting and relationship to magmatism, *in* Ernst, W.G., ed., Metamorphism and crustal evolution, western coterminous United States: Rubey Volume 7: Englewood Cliffs, New Jersey, Prentice-Hall, p. 649–682.

Min, K., Mundil, R., Renne, P.R., and Ludwig, K.R., 2000, A test for systematic errors in $^{40}Ar/^{39}Ar$ geochronology through comparison with U/Pb analysis of a 1.1 Ga rhyolite: Geochimica et Cosmochimica Acta, v. 64, p. 73–98, doi:10.1016/S0016-7037(99)00204-5.

Mitra, S., 1990, Fault-propagation folds: Geometry, kinematic evolution, and hydrocarbon traps: American Association of Petroleum Geologists Bulletin, v. 74, p. 921–945.

Nolan, T.B., 1962, The Eureka mining district, Nevada: U.S. Geological Survey Professional Paper 406, 78 p.

Nolan, T.B., Merriam, C.W., and Brew, D.A., 1971, Geologic map of the Eureka quadrangle, Eureka and White Pine counties, Nevada: U.S. Geological Survey Miscellaneous Investigations Series Map I-612, scale 1:31,680, 8 p.

Nolan, T.B., Merriam, C.W., and Blake, M.C., Jr., 1974, Geologic map of the Pinto Summit quadrangle, Eureka and White Pine counties, Nevada: U.S. Geological Survey Miscellaneous Investigations Series Map I-793, scale 1:31,680, 14 p.

Oldow, J.S., 1983, Tectonic implications of a late Mesozoic fold and thrust belt in northwestern Nevada: Geology, v. 11, p. 542–546, doi:10.1130/0091-7613(1983)11<542:TIOALM>2.0.CO;2.

Oldow, J.S., 1984, Evolution of a late Mesozoic back-arc fold and thrust belt, northwestern Great Basin, U.S.A: Tectonophysics, v. 102, p. 245–274, doi:10.1016/0040-1951(84)90016-7.

Oldow, J.S., Bally, A.W., Ave Lallemant, H.G., and Leeman, W.P., 1989, Phanerozoic evolution of the North American Cordillera: United States and Canada, *in* Bally, A.W., and Palmer, A.R., eds., The geology of North America—An overview: Boulder, Colorado, Geological Society of America, Geology of North America, v. A, p. 139–232.

Palmer, A.R., 1960, Identification of the Dunderberg shale of Late Cambrian age in the eastern Great Basin: U.S. Geological Survey Professional Paper 400-B, p. B289–B290.

Perry, W.J., and Dixon, G.L., 1993, Structure and time of deformation in the central Pancake Range, a geologic reconnaissance, *in* Gillespie, C.W., ed., Structural and stratigraphic relationships of Devonian reservoir rocks, east-central Nevada: Nevada Petroleum Society 1993 Field Conference Guidebook NPS 07, p. 123–132.

Poole, F.G., 1974, Flysch deposits of Antler foreland basin, western United States, *in* Dickinson, W.R., ed., Tectonics and sedimentation: SEPM (Society of Economic Paleontologists and Mineralogists) Special Publication 22, p. 58–82.

Poole, F.G., and Sandberg, C.A., 1977, Mississippian paleogeography and tectonics of the western United States, *in* Stewart, J.H., et al., eds., Paleozoic paleogeography of the western United States: Los Angeles, Pacific Section, SEPM (Society of Economic Paleontologists and Mineralogists), p. 67–85.

Potter, C.J., Dubiel, R.F., Snee, L.W., and Good, S.C., 1995, Eocene extension of early Eocene lacustrine strata in a complexly deformed Sevier-Laramide hinterland, northwest Utah and northeast Nevada: Geology, v. 23, p. 181–184, doi:10.1130/0091-7613(1995)023<0181:EEOEEL>2.3.CO;2.

Ransom, K.L., and Hansen, J.B., 1993, Cretaceous transpressional deformation, Eureka County, Nevada, *in* Gillespie, C.W., ed., Structural and stratigraphic relationships of Devonian reservoir rocks, east-central Nevada: Nevada Petroleum Society 1993 Field Conference Guidebook NPS 07, p. 89–104.

Roeder, D., 1989, Thrust belt of central Nevada, Mesozoic compressional events, and the implication for petroleum prospecting, *in* Garside, L.J., and Shaddrick, D.R., eds., Compressional and extensional structural styles in the northern Basin and Range, Nevada: Seminar Proceedings: Nevada Petroleum Society, p. 21–34.

Ross, R.J., Jr., 1970, Ordovician brachiopods, trilobites, and stratigraphy in eastern and central Nevada: U.S. Geological Survey Professional Paper 639, 103 p.

Royse, F., Jr., Warner, M.A., and Reese, D.L., 1975, Thrust belt structural geometry and related stratigraphic problems Wyoming-Idaho-northern Utah, *in* Bolyard, D.W., ed., Deep drilling frontiers of the central Rocky Mountains: Denver, Colorado, Rocky Mountain Association of Geologists, p. 41–54.

Samson, S.D., and Alexander, E.C., Jr., 1987, Calibration of the interlaboratory $^{40}Ar/^{39}Ar$ dating standard, MMhb-1: Chemical Geology, v. 66, p. 27–34, doi:10.1016/0168-9622(87)90025-X.

Schalla, R.A., 1978, Paleozoic stratigraphy of the Southern Mahogany Hills, Eureka County, Nevada [M.S. thesis]: Corvallis, Oregon State University, 118 p.

Simonds, G.G., 1997, Geology and structural patterns for the Mountain Boy Range, Eureka County, Nevada [M.S. thesis]: Rapid City, South Dakota School of Mines and Technology, 75 p.

Smith, J.F., and Ketner, K.B., 1976, Stratigraphy of Post-Paleozoic rocks and summary of resources in the Carlin-Pinon Range area, Nevada: USGS Professional Paper 867-B, 48 p.

Smith, J.F., Jr., and Ketner, K.B., 1977, Tectonic events since early Paleozoic in the Carlin–Pinon Range area, Nevada: U.S. Geological Survey Professional Paper 876C, 18 p.

Snoke, A.W., and Miller, D.M., 1988, Metamorphic and tectonic history of the northeastern Great Basin, *in* Ernst, W.G., ed., Metamorphism and crustal evolution, western coterminous United States: Rubey Volume 7: Englewood Cliffs, New Jersey, Prentice-Hall, p. 606–648.

Speed, R.C., and Sleep, N., 1982, Antler orogeny and foreland basin: A model: Geological Society of America Bulletin, v. 93, p. 815–828, doi:10.1130/0016-7606(1982)93<815:AOAFBA>2.0.CO;2.

Speed, R.C., Elison, M.W., and Heck, R.R., 1988, Phanerozoic tectonic evolution of the Great Basin, *in* Ernst, W.G., editor, Metamorphism and crustal evolution of the western United States: Rubey Volume 7: Englewood Cliffs, New Jersey, Prentice-Hall, p. 572–605.

Steiger, R.H., and Jäger, E., 1977, Subcommission on geochronology: Convention on the use of decay constants in geo- and cosmochronology: Earth and Planetary Science Letters, v. 36, p. 359–362, doi:10.1016/0012-821X(77)90060-7.

Stewart, J.H., 1962, Variable facies of the Chainman and Diamond Peak Formations in western White Pine County, Nevada: U.S. Geological Survey Professional Paper 450-C, p. C57–C60.

Stewart, J.H., and Carlson, J.E., 1978, Geologic map of Nevada: U.S. Geological Survey, Nevada Bureau of Mines and Geology, scale 1:500,000.

Stewart, J.H., and Poole, F.G., 1974, Lower Paleozoic and uppermost Precambrian Cordilleran miogeocline, Great Basin, western United States, *in* Dickinson, W.R., ed., Tectonics and sedimentation: SEPM (Society of Economic Paleontologists and Mineralogists) Special Publication 22, p. 28–57.

Suppe, J., 1983, Geometry and kinematics of fault-bend folding: American Journal of Science, v. 283, p. 684–721, doi:10.2475/ajs.283.7.684.

Taylor, W.J., Bartley, J.M., Fryxell, J.E., Schmitt, J., and Vandervoort, D.S., 1993, Mesozoic central Nevada thrust belt, *in* Lahren, M.M., et al., eds., Crustal evolution of the Great Basin and the Sierra Nevada: Geological Society of America Cordilleran/Rocky Mountain Sections Field Trip Guidebook: Reno, University of Nevada Mackay School of Mines, p. 57–96.

Taylor, W.J., Bartley, J.M., Martin, M.W., Geissman, J.W., Walker, J.D., Armstrong, P.A., and Fryxell, J.E., 2000, Relations between hinterland and foreland shortening: Sevier orogeny, central North American Cordillera: Tectonics, v. 19, p. 1124–1143, doi:10.1029/1999TC001141.

Thorman, C.H., Ketner, K.B., Brooks, W.E., Snee, L.W., and Zimmermann, R.A., 1991, Late Mesozoic–Cenozoic tectonics in northeastern Nevada, *in* Raines, G.L., et al., eds., Geology and ore deposits of the Great Basin: Symposium proceedings: Reno, Geological Society of Nevada, p. 25–45.

Thorman, C.H., Ketner, K.B., and Peterson, F., 1992, The Middle to Late Jurassic Elko orogeny in eastern Nevada and western Utah: Geological Society of America Abstracts with Programs, v. 24, p. 66.

Trexler, J.H., Cashman, P.H., Snyder, W.S., and Davydov, V.I., 2004, Late Paleozoic tectonism in Nevada: Timing, kinematics, and tectonic significance: Geological Society of America Bulletin, v. 116, p. 525–538, doi:10.1130/B25295.1.

U.S. Geological Survey, 2006, Quaternary fault and fold database for the United States: http://earthquake.usgs.gov/regional/qfaults/ (accessed June 21, 2012).

Van Buer, N.J., Miller, E.L., and Dumitru, T.A., 2009, Early Tertiary paleogeologic map of the northern Sierra Nevada batholith and the northwestern Basin and Range: Geology, v. 37, p. 371–374, doi:10.1130/G25448A.1.

Vandervoort, D.S., 1987, Sedimentology, provenance, and tectonic implications of the Cretaceous Newark Canyon Formation, east-central Nevada [M.S. thesis]: Bozeman, Montana State University, 145 p.

Vandervoort, D.S., and Schmitt, J.G., 1990, Cretaceous to early Tertiary paleogeography in the hinterland of the Sevier thrust belt, east-central Nevada: Geology, v. 18, p. 567–570, doi:10.1130/0091-7613(1990)018<0567:CTETPI>2.3.CO;2.

Villien, A., and Kligfield, R.M., 1986, Thrusting and synorogenic sedimentation in central Utah, *in* Peterson, J.A., ed., Paleotectonics and sedimentation in the Rocky Mountain region, United States: American Association of Petroleum Geologists Memoir 41, p. 281–308.

Wiltschko, D.V., and Dorr, J.A., Jr., 1983, Timing of deformation in overthrust belt and foreland of Idaho, Wyoming, and Utah: American Association of Petroleum Geologists Bulletin, v. 67, p. 1304–1322.

Wyld, S.J., 2002, Structural evolution of a Mesozoic back-arc fold-and-thrust belt in the U.S. Cordillera: New evidence from northern Nevada: Geological Society of America Bulletin, v. 114, p. 1452–1468, doi:10.1130/0016-7606(2002)114<1452:SEOAMB>2.0.CO;2.

Wyld, S.J., Rogers, J.W., and Wright, J.E., 2001, Structural evolution within the Luning-Fencemaker fold-thrust belt, Nevada: Progression from back-arc basin collapse to intra-arc shortening: Journal of Structural Geology, v. 23, p. 1971–1995, doi:10.1016/S0191-8141(01)00042-6.

Xiao, H., and Suppe, J., 1992, Origin of rollover: American Association of Petroleum Geologists Bulletin, v. 76, p. 509–529.